Heat stress induces ferroptosis-like cell death in plants

Ayelén Mariana Distéfano,[1]* María Victoria Martin,[1]* Juan Pablo Córdoba,[1] Andrés Martín Bellido,[1] Sebastián D'Ippólito,[1] Silvana Lorena Colman,[1] Débora Soto,[1] Juan Alfredo Roldán,[1] Carlos Guillermo Bartoli,[2] Eduardo Julián Zabaleta,[1] Diego Fernando Fiol,[1] Brent R. Stockwell,[3,4] Scott J. Dixon,[5] and Gabriela Carolina Pagnussat[1]

[1]Instituto de Investigaciones Biológicas, Consejo Nacional de Investigaciones Científicas y Técnicas (CONICET), Universidad Nacional de Mar del Plata, 7600 Mar del Plata, Argentina
[2]Instituto de Fisiología Vegetal, Facultad de Ciencias Naturales, Universidad Nacional de La Plata Centro Científico Tecnológico La Plata CONICET, 1900 La Plata, Argentina
[3]Department of Biological Sciences and [4]Department of Chemistry, Columbia University, New York, NY 10027
[5]Department of Biology, Stanford University, Stanford, CA 94305

In plants, regulated cell death (RCD) plays critical roles during development and is essential for plant-specific responses to abiotic and biotic stresses. Ferroptosis is an iron-dependent, oxidative, nonapoptotic form of cell death recently described in animal cells. In animal cells, this process can be triggered by depletion of glutathione (GSH) and accumulation of lipid reactive oxygen species (ROS). We investigated whether a similar process could be relevant to cell death in plants. Remarkably, heat shock (HS)–induced RCD, but not reproductive or vascular development, was found to involve a ferroptosis-like cell death process. In root cells, HS triggered an iron-dependent cell death pathway that was characterized by depletion of GSH and ascorbic acid and accumulation of cytosolic and lipid ROS. These results suggest a physiological role for this lethal pathway in response to heat stress in *Arabidopsis thaliana*. The similarity of ferroptosis in animal cells and ferroptosis-like death in plants suggests that oxidative, iron-dependent cell death programs may be evolutionarily ancient.

Introduction

In eukaryotes, regulated cell death (RCD) is an active mechanism essential for development, immune responses, and many pathophysiological processes (Hakem et al., 1998; Yoshida et al., 1998; Lindsten et al., 2000; Van Hautegem et al., 2015). In animals, cell death was traditionally classified into three categories, based on the morphological features exhibited by cells during the death process, as apoptotic, autophagic, or necrotic (Kroemer et al., 2009). In recent years, this tripartite classification scheme has been challenged by the discovery of new forms of cell death that differ from these canonical categories, such as pyroptosis and necroptosis (Bergsbaken et al., 2009; Christofferson and Yuan, 2010). Most recently, a new form of cell death that was shown to be morphologically, biochemically, and genetically distinct from apoptosis, necrosis, and autophagy was described in cancer cells, in kidney tissue, and in the nervous system. This type of cell death was named ferroptosis, as it is dependent on intracellular iron, which is required for the accumulation of toxic lipid reactive oxygen species (ROS; Yang and Stockwell, 2008; Dixon et al., 2012; Friedmann Angeli et al., 2014; Linkermann et al., 2014; Skouta et al., 2014; Yang et al., 2014). A defining feature of ferroptosis is that it can be prevented by treatment of cells with iron-chelating agents, such as deferoxamine or ciclopirox olamine (CPX), or with lipophilic antioxidants, such as ferrostatin 1 (Fer-1) or vitamin E (Yagoda et al., 2007; Yang and Stockwell, 2008; Dixon et al., 2012; Skouta et al., 2014; Yang et al., 2014). Although the specific role of iron in ferroptosis remains unclear, it is unlikely to be explained by a simple increase in iron-catalyzed ROS production (i.e., Fenton chemistry), as cell death induced by peroxide is in many aspects different from ferroptosis (Dixon et al., 2012).

In plants, RCD mechanisms play critical roles during several developmental processes, such as megasporogenesis, fertilization, embryogenesis, development of tracheary elements, and regulation of leaf shape (Gunawardena et al., 2004; Drews and Koltunow, 2011; Bollhöner et al., 2012; Choi, 2013). Additionally, abiotic stresses, such as salt stress, drought, and nutrient starvation, are able to induce plant cell death (Liu et al., 2009). Plant cells do not undergo apoptosis as defined by classic

*A.M. Distéfano and M.V. Martin contributed equally to this paper.

Correspondence to Gabriela Carolina Pagnussat: gpagnussat@mdp.edu.ar; or Scott J. Dixon: sjdixon@stanford.edu

M.V. Martin's present address is Instituto de Investigaciones en Biodiversidad y Biotecnología, Fundación para Investigaciones Biológicas Aplicadas, 3103 Mar del Plata, Argentina.

Abbreviations used: AA, ascorbic acid; CPX, ciclopirox olamine; DIC, differential interference contrast; DPI, diphenyleneiodonium; Fer-1, ferrostatin 1; GSH, glutathione; HS, heat shock; HSP, HS protein; mitoSOX, mitochondrial superoxide; Nec-1, necrostatin 1; NOX, NADPH oxidase; PCD, programmed cell death; PUFA, polyunsaturated fatty acid; RCD, regulated cell death; ROS, reactive oxygen species; TEM, transmission EM.

The Rockefeller University Press $30.00
J. Cell Biol. Vol. 216 No. 2 463–476
https://doi.org/10.1083/jcb.201605110

morphological features observed in animal cells. The rigid plant cell wall prevents the cells from breaking into apoptotic bodies, and even though protoplasts are known to shrink in response to diverse abiotic stresses, they do not further fragment into discrete bodies. Thus, a recent classification of plant programmed cell death (PCD) stated that the use of the term "apoptosis-like" is not justified in plants, although it remains a subject of debate (van Doorn et al., 2011).

Vacuoles may be involved in a specific form of plant cell death. A large vacuolar system occupies most of the plant cell volume (Marty, 1999). These vacuoles have important functions during a plant-specific type of cell death, termed vacuolar cell death, that involves a gradual decrease in the cytoplasm volume and formation of small lytic vacuoles, resembling autophagy (Jones, 2001). Several *A. thaliana* autophagy genes (*ATG*) have been implicated in this type of cell death and were first identified based on sequence similarity to yeast autophagy genes (Xie and Klionsky, 2007). Remarkably, mitochondria and other organelles remain intact until the final stages of vacuolar cell death, which involves tonoplast rupture, disassembly of the nuclear envelope, and nuclear segmentation (van Doorn et al., 2011). Vacuolar cell death is associated with several developmental pathways, including aerenchyma formation, leaf remodeling, and xylem differentiation (Drew et al., 2000; Gunawardena, 2008; Courtois-Moreau et al., 2009; Kwon et al., 2010), and has also been linked to plant responses to environmental stress conditions and to leaf senescence (Liu et al., 2009; Kariya et al., 2013).

In this work, we examined whether iron-dependent, oxidative processes similar to those recently described to occur during ferroptosis in animal cells could be relevant to plant cell death during development or after abiotic stress. Remarkably, ferroptosis was implicated in the RCD that follows heat shock (HS) stress, but not in several other cell death events. These results show that a group of morphological and biochemical features that are specific for ferroptosis are present in *Arabidopsis* roots in response to HS and suggest an underlying similarity between ferroptosis-like plant cell death and animal cell death.

Results

An oxidative, iron-dependent cell death is triggered in response to HS in plants

Diverse environmental stresses, such as salt stress, high temperatures, drought, and nutrient starvation, are able to induce cell death in plants (Liu et al., 2009). Stress-induced cell death can be studied by following the response to HS, hydrogen peroxide (H_2O_2), and salt (NaCl) stress in cell suspensions and root hairs (Reape and McCabe, 2008; Blanvillain et al., 2011; Hogg et al., 2011). A 10-min heat treatment at 55°C (55°C HS) triggers RCD in *A. thaliana*, whereas exposure to higher temperatures promotes necrosis (Reape and McCabe, 2008; Blanvillain et al., 2011). The mechanism involved in the cell death triggered by moderate heat (i.e., 55°C HS) is not clear, but is known to involve the accumulation of ROS (Hogg et al., 2011). We hypothesized that processes related to the iron-dependent, oxidative ferroptotic pathway described in animal cells could be relevant to stress-induced cell death in *A. thaliana.* To test this hypothesis, diverse lethal treatments were performed in the presence of two small-molecule ferroptosis inhibitors discovered and characterized in animal cells: the lipophilic antioxidant Fer-1 and the membrane-permeable iron chelator CPX (Dixon et al., 2012). CPX has a very high affinity for iron, comparable to that of deferoxamine (Linden et al., 2003). Its higher lipophilicity, specificity, and availability make this iron chelator a very useful tool in cell biology studies (Kuriki et al., 1975).

When 6-d-old seedlings were preincubated for 16 h before HS with 1 µM Fer-1 or 10 µM CPX, the death of root hairs triggered by 55°C HS, as assayed by Sytox green nucleic acid stain, was significantly prevented (Fig. 1 a). In contrast, neither Fer-1 nor CPX prevented cell death triggered by 77ºC H_2O_2 or NaCl treatments (Fig. 1 a), suggesting that ferroptosis inhibitors specifically block cell death triggered by 55°C HS. Necrostatin 1 (Nec-1), a potent inhibitor of a different nonapoptotic cell death pathway in animal cells, RIPK1-mediated, did not prevent cell death triggered by HS at either 55°C or 77°C (Fig. S1 a). This suggests that necroptosis is not involved in HS-induced death in plant cells.

In plants, RCD is calcium dependent in numerous systems and tissues (Ma and Berkowitz, 2007); thus, the effect of calcium chelators was studied in 55°C HS–triggered cell death. Whereas at 6 h after treatment, ∼70% of the root hairs in *A. thaliana* roots were dead, only ∼10% died when cotreated with the calcium chelator EGTA, a value comparable to that seen in untreated roots, suggesting that influx of calcium from the extracellular space is required for HS-induced, iron-dependent cell death in plants (Fig. 1 b). In addition, dose–response curves were constructed in which we measured the ability of Fer-1 and two structural analogues to prevent HS-induced cell death in roots. Overall, plant cells were more sensitive to Fer-1 and structurally related compounds than human cells: whereas Fer-1 had an EC_{50} of 60 nM in cancer cells (Dixon et al., 2012), the EC_{50} in plant cells was 2.5 pM (Fig. 1 c). Similarly, the two Fer-1 analogues tested (SRS9-01 and SRS8-24) showed lower EC_{50} values, and the tendency observed was equivalent to the one described for these analogues in tumor cells (Dixon et al., 2012). Substitution of the primary aromatic amine, which is essential for antioxidant function (SRS9-01 and SRS8-24) resulted in less protection against cell death, as reported for animal cells (Dixon et al., 2012; Skouta et al., 2014). Incubation of plants with an exogenous source of iron (200 µM FeNa-EDTA) did not potentiate the 55°C HS–induced death in root cells. Likewise, the application of other divalent metal ions (e.g., Cu^{2+} and Mn^{2+}) did not have any effect on 55°C HS–induced cell death (Fig. S1 b). One possibility is that the requirement of iron was already fulfilled in planta, and thus cell death was occurring at its maximum rate already. Alternatively, exogenous iron may not reach the intracellular sites or enzymes that promote cell death under these conditions.

Analyses of root hair morphology using differential interference contrast (DIC) microscopy showed that 55°C HS produced cytoplasmic retraction and strong nuclear Sytox green staining (Fig. 2 a). No cytoplasmic retraction was observed in root hairs treated at 77°C, and neither Fer-1 nor CPX was protective at this temperature (Fig. 2 a). Root hairs treated with H_2O_2 or NaCl showed partial cytoplasmic retraction and cell death that was not prevented by Fer-1 or CPX (Fig. 2 a). Using transmission EM (TEM) on root cortical cells, we confirmed that after 6 h, 55°C HS resulted in cytoplasmic retraction, and we observed the presence of numerous lytic vacuoles and shrunken and less abundant mitochondria showing a dark (condensed) matrix. In tumor cells, the only distinctive morphological characteristic of ferroptotic cells was the presence of

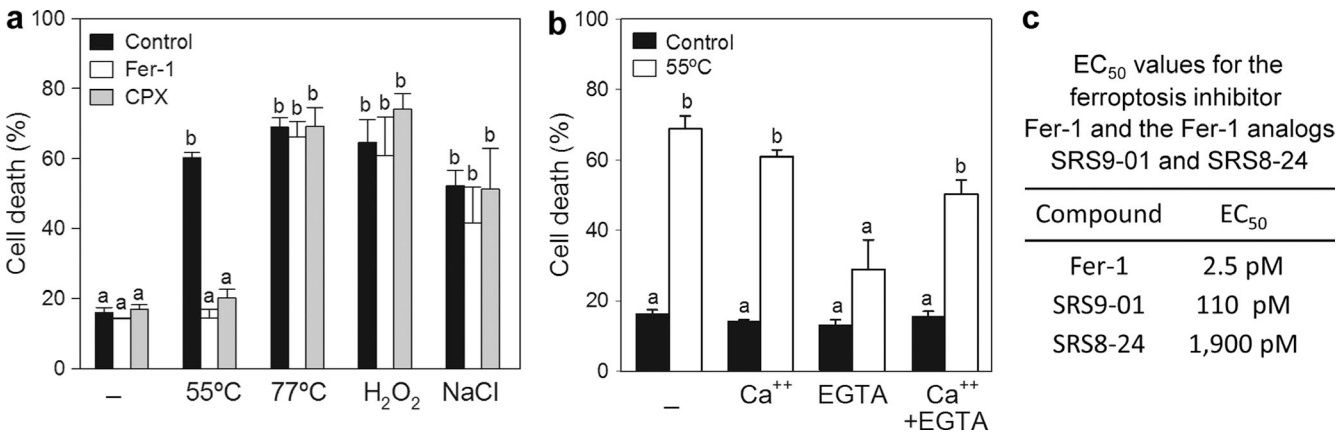

Figure 1. **Ferroptosis inhibitors prevent PCD induced by 55°C HS in *Arabidopsis* root hairs.** (a) 6-d-old seedlings were preincubated with 1 µM Fer-1 (white bars), 10 µM CPX (gray bars), or DMSO (black bars). Cell death was induced by treating roots at 55°C or 77°C for 10 min, with H_2O_2 for 6 h, or with NaCl for 16 h. (b) 6-d-old seedlings were preincubated with $CaCl_2$ for 16 h, with 1 mM EGTA for 2 h, or with EGTA for 2 h and then with $CaCl_2$ for 16 h before inducing cell death by treating roots at 55°C for 10 min. (a and b) Root hairs were stained with Sytox green, and Sytox-positive cells (interpreted as dead cells) and Sytox-negative cells were quantified. Results are expressed as a percentage of dead cells. Data are the mean + SEM of three independent experiments. Bars with different letters denote statistical difference (one-way analysis of variance, $P < 0.05$). Also see Fig. S1. (c) 6-d-old seedlings were preincubated with Fer-1 analogues SR9-01 and SRS8-24 before treatment at 55°C. Root hairs were stained with Sytox green, and the number of Sytox-positive cells (interpreted as dead cells) and Sytox-negative cells was quantified to obtain the EC_{50} of those compounds.

smaller mitochondria that showed increased membrane density compared with normal cells (Yagoda et al., 2007; Dixon et al., 2012). Plant cells from roots treated at 77°C showed no cytoplasmic retraction, and the presence of mitochondria was rare, as was the presence of lytic vacuoles (Fig. 2 b). To know how mitochondrial morphology was affected after HS, we measured mitochondria at different times after HS using MitoTracker green and confocal microscopy. As shown in Fig. 2 c, mitochondrial planar area increased during the first hours after 55°C HS, consistent with mitochondrial swelling in cells undergoing cell death. After 6 h of 55°C HS, mitochondria were slightly smaller than in control cells. Thus, 55°C HS resulted in mitochondrial morphological changes that mimic those observed in cancer cells undergoing ferroptosis, and in the accumulation of lytic vacuoles that are not observed in cancer cells.

Using Sytox green and confocal microscopy, we investigated how the different cell types that compose the roots were dying over time after 55°C HS treatment (Videos 1, 2, 3, and 4). We observed that root hairs and cells composing the main root, principally those related to the central cylinder, were dying during the first hours after exposure to 55°C. Interestingly, the vast majority of iron in the root was reported to locate within the central cylinder, whereas only very small amounts of iron can be detected in the epidermis and cortex (Kuriki et al., 1975).

55°C HS triggers ROS accumulation and depletion of endogenous antioxidants

In tumor cells, ferroptosis is characterized by the iron-dependent accumulation of lethal cytosolic and lipid ROS. In these cells, the accumulation of cytosolic and lipid ROS is prevented by iron chelation (Dixon et al., 2012). To investigate whether a similar process takes place in *Arabidopsis*, we measured changes in cytosolic and lipid ROS using the fluorescent probes H_2DCFDA and C11-BODIPY$^{581/591}$, respectively, after inducing cell death with a 55°C HS in *A. thaliana* roots and in cell suspensions. No change in lipid ROS was detected in root cells under these conditions, perhaps because of the limited sensitivity of the C11-BODIPY dye. However, H_2DCFDA fluorescence increased as early as 30 min after treatment and preceded cell death (Fig. 3 a). ROS were detected at high levels until 6 h after HS, when the cells died (Fig. 3 b). ROS accumulation and cell death were both prevented by cotreatment with CPX or Fer-1. When cell death was induced in *A. thaliana* cell suspensions, both cytosolic and lipid ROS were increased (Fig. S2). These increases were suppressed by cotreatment with CPX or Fer-1 (Fig. S2). To test whether mitochondrial ROS were involved in this type of cell death, mitochondrial superoxide (mitoSOX)–sensitive ROS production was measured after HS. No increase in mitoSOX was detected either in *Arabidopsis* root hairs or in cell suspensions (Figs. S2 and S3).

The mechanism of lipid peroxidation during ferroptosis was recently reported to involve peroxidation of polyunsaturated fatty acids (PUFAs) at the bis-allylic position in human cells. Pretreatment of cancer cells with PUFAs containing the heavy hydrogen isotope deuterium at the site of peroxidation (D-PUFAs) prevented PUFA peroxidation, blocking ferroptosis (Yang et al., 2016a). Likewise, we observed that preincubation with 8 µM D4-linoleate (16 h) protected plants against 55°C HS but not against 77°C HS (Fig. 3 e). Together, these results suggested that plant cells exposed to HS undergo an oxidative, iron-dependent form of cell death similar to ferroptosis observed in animal cells.

To investigate another possible source of ROS that might be involved in 55°C HS–induced cell death, *A. thaliana* roots and cells were exposed to 55°C HS in the presence of diphenyleneiodonium (DPI). DPI is an inhibitor of NADPH oxidase (NOX) and other flavo-enzymes such as NO synthase and xanthine oxidase (Wind et al., 2010). DPI treatment prevented the increase in ROS after HS (Fig. S2). Thus, as in human tumor cells (Dixon et al., 2012), HS-induced cell death in *A. thaliana* does not involve mitoSOX production and may involve NOX enzymes and lipid peroxidation.

Reduced glutathione (GSH) and ascorbic acid (AA) are important redox buffers in eukaryotic cells (Pavet et al., 2005; Kranner et al., 2006; Franco and Cidlowski, 2012). AA depletion has been linked to ROS accumulation and cell death associated with plant defense responses during pathogen attack and senescence (Pavet et al., 2005). GSH depletion is considered a

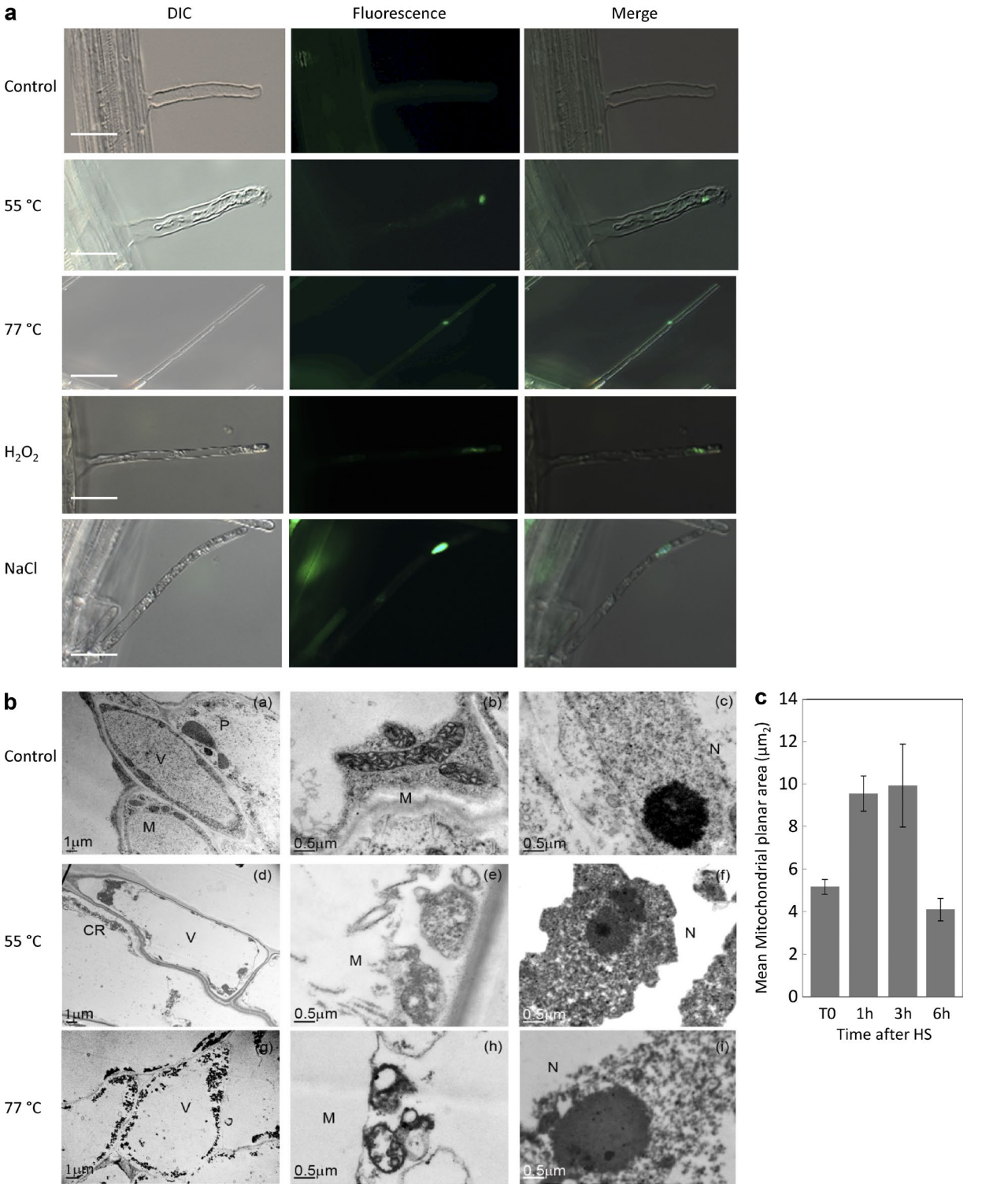

Figure 2. **Morphology of root cells after inducing cell death.** (a) 6-d-old seedlings were treated with DMSO (control), 55°C, or 77°C for 10 min or with H_2O_2 for 6 h or NaCl for 16 h. Root hairs were stained with Sytox green 6 h after HS or right after H_2O_2 or NaCl treatments. The appearance of cells was examined using DIC microscopy or fluorescent microscopy. Bars, 50 µm. (b) TEM micrographs of *Arabidopsis* root cortical cells 6 h after HS: (a–c), root cells from a nonstressed (control) root; (d–f) root cells from a 55°C-treated root, showing cytoplasmic retraction and shrunken, abnormal mitochondria; and (g–i) root cells from a 77°C-treated root, showing mitochondria with a light matrix and very few cristae. V, vacuole; N, nuclei; M, mitochondria; P, plastids; CR, cytoplasmic retraction. (c) Size of mitochondria in roots of plants submitted to HS. Roots were stained with MitoTracker green FM, and mitochondrial images were obtained using confocal microscopy at the times indicated. Quantification of mitochondrial area was performed using the Mito-Morphology macro for ImageJ software (T0, n = 93; 2 h, n = 58; 3 h, n = 33; 6 h, n = 62).

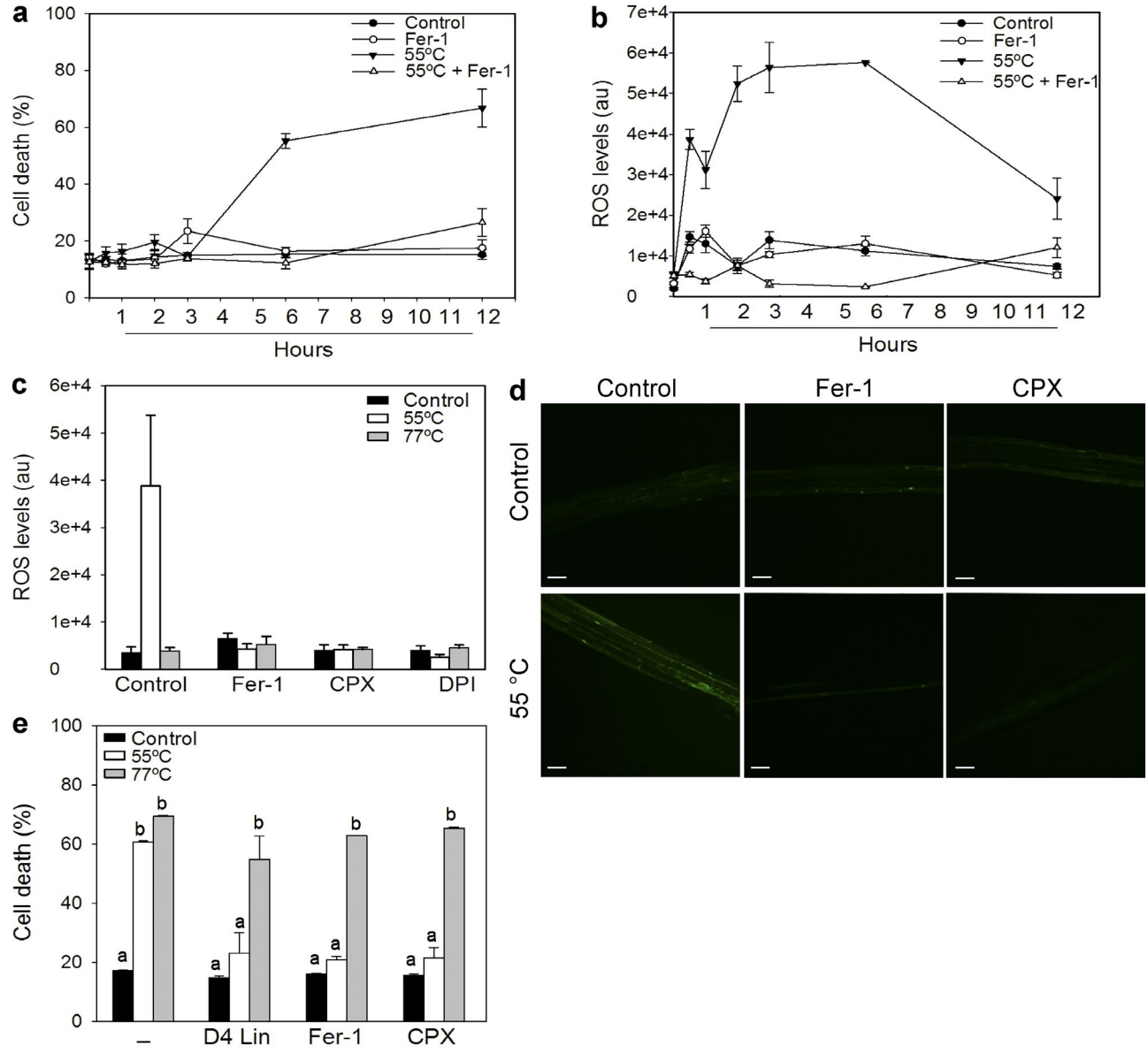

Figure 3. **Ferroptosis inhibitors prevent cell death and ROS accumulation induced by HS in *Arabidopsis* roots.** 6-d-old seedlings were preincubated with 1 µM Fer-1, 10 µM CPX, or DMSO (Control) as indicated. Cell death was induced by treating roots at 55°C for 10 min. (a) Kinetics of cell death induced by a 55°C HS. (b) Kinetics of ROS levels induced after a 55°C HS treatment. ROS accumulation in roots was detected by using the H_2DCFDA probe. (c) ROS production is mediated by NOX activity and prevented by cotreatment with ferroptosis inhibitors or cotreatment with the NOX inhibitor DPI. Data are the mean ± SEM of three independent experiments. (d) Representative confocal images showing ROS detected by the H_2DCFDA probe in *A. thaliana* roots. Bars, 50 µm. (e) Suppression of cell death after a 55°C HS by D4-linoleate (D4 Lin). 6-d-old seedlings were preincubated with 1 µM Fer-1, 10 µM CPX, 8 µM D4-linoleate, or DMSO (control) as indicated. Cell death was induced by treating roots at 55°C or 77°C for 10 min. (a and e) Root hairs were stained with Sytox green, and Sytox-positive (interpreted as dead cells) and Sytox-negative cells were quantified. Results are expressed as a percentage of dead cells. Bars with different letters denote statistical difference (one-way analysis of variance, $P < 0.05$).

central event that activates cell death pathways in both animal and plant cells (Kranner et al., 2006; Franco and Cidlowski, 2012). In mammalian cells, class I ferroptosis-inducing agents are thought to trigger ferroptosis by depleting the cell of GSH (Skouta et al., 2014; Yang et al., 2014). In plants, it is likely that AA levels are affected as well. We therefore measured the levels of GSH and AA in root tissues after 55°C HS. Both total GSH and AA concentrations declined after HS (Fig. 4, a and b). An increase in the fraction of the oxidized AA was also detected after HS (Fig. 4 a). These effects were not reverted by cotreatment with Fer-1 or CPX, demonstrating that GSH and AA depletion is upstream of lipid ROS accumulation, as in animal cells (Dixon et al., 2012; Skouta et al., 2014; Yang et al., 2014). To determine whether GSH depletion was necessary for the ferroptotic-like death observed upon 55°C HS in plant roots, plants were cotreated with GSH, which can be taken up by plant cells (Schneider et al., 1992; Jamai et al., 1996; Zhang et al., 2004). Notably, when GSH was added to the culture medium, HS-induced cell death was prevented (Fig. 4 c). Additionally, we determined that GSH depletion was sufficient to trigger cell death, as *Arabidopsis* roots treated with L-buthionine-(S,R)-sulfoximine, a specific inhibitor of GSH biosynthesis, showed ~50% of cell death after 4 d of treatment (Fig. 4 d). Thus, GSH depletion is critical for HS-induced cell death in

a

Ascorbic acid (AA) content in Arabidopsis roots

Treatment	Reduced AA nmol g^{-1}FW	Total AA	Redox status (% of oxidized AA)
Control	107±40	154±40	30.5
Fer	55±20	78±22	29.5
CPX	100.6±57	138.3±78	27.5
55°C	21.5±3.3	58.8±6	62.0
55°C+Fer-1	23.6±6.7	54.5±8	56.6
55°C+CPX	41.45±36	68.7±46	54.25
77°C	2.6±1.34	13±2.9	80.0
77°C+Fer-1	2.6±2.2	16±7	83.7
77°C+CPX	5.65±2.65	22.45±1.05	69.95

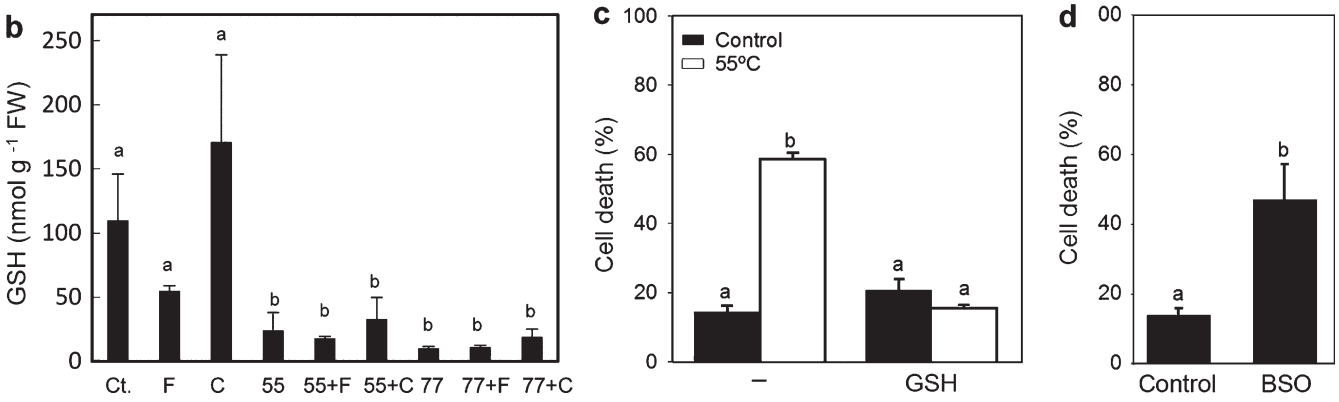

Figure 4. **Plant ferroptosis involves GSH and AA oxidation and depletion.** (a) AA levels in *A. thaliana* roots before or after treatment at 55°C or 77°C with or without the ferroptosis inhibitors Fer-1 and CPX. FW, fresh weight. (b) GSH levels in *A. thaliana* roots before (Ct., control) or after treatment at 55°C (55) or at 77°C with or without the ferroptosis inhibitors Fer-1 (F) and CPX (C). Data are the mean ± SEM of three independent experiments. Different letters denote statistical difference (one-way analysis of variance, $P < 0.05$). (c) 6-d-old seedlings were preincubated with 100 µM GSH or DMSO overnight (16 h). Cell death was induced by treating roots at 55°C. (d) *Arabidopsis* seedlings were grown in control plates or 10 µM L-buthionine-(S,R)-sulfoximine (BSO)–supplemented plates. 6-d-old seedlings were analyzed. (c and d) Root hairs were stained with Sytox green, and Sytox-positive (interpreted as dead cells) and Sytox-negative cells and the number of dead and living root hairs was quantified. Results are expressed as a percentage of dead cells. Data are mean ± SEM of three independent experiments. Different letters denote statistical difference (one-way analysis of variance, $P < 0.05$).

plants, probably by compromising the ROS-scavenging capacity of the cell. Altogether, these results suggest that plant cells can also undergo an oxidative, iron-dependent type of cell death similar to ferroptosis in animal cells.

55°C HS–induced death requires caspase-like activity but does not result in DNA fragmentation

Despite the absence of plant orthologues for caspase genes, proteases with caspase-like enzymatic activities are required for plant cell death (Danon et al., 2004; Ge et al., 2016). To assess whether caspase-like activity is involved in cell death triggered by HS in *Arabidopsis*, we studied the effect of preincubation with the caspase-3 inhibitor Ac-DEVD-CHO (CHO). We observed that preincubation with CHO partially reduced the percentage of cell death triggered by 55°C HS but not 77°C HS (Fig. S4 a). This suggested that a caspase-like activity was involved in the pathway triggered after 55°C exposure. To study another aspect linked to apoptosis-like cell death, we assessed DNA fragmentation by using TUNEL assays (Fig. S4 b). No TUNEL-positive nuclei were detected in roots 6 h after the initiation of 55°C HS. Although we cannot exclude DNA fragmentation as a late outcome for this cell death pathway, these results suggest that it might not take place at least at 6 h after HS, when cell death is already detected in root tissues.

Fer-1 and CPX do not prevent reproductive or developmental cell death

The potential involvement of ferroptosis-like cell death during reproductive development was investigated. *A. thaliana* inflorescences were treated with Fer-1 or CPX, and pistils composing the inflorescence, ranging in size between 1 and 8 mm, were examined for two key events involving cell death: (1) megaspore cell death that occurs as the final step of megasporogenesis and (2) synergid cell death, the death of the cells that receive the pollen tube during fertilization (Christensen et al., 2002; Sandaklie-Nikolova et al., 2007). After treatment, the cleared ovules were examined for defects in megasporogenesis or fertilization (see Materials and methods for details). However, no abnormalities were detected, suggesting that ferroptosis might not be involved in these developmental cell death processes (Fig. S5, a–c).

During vascular differentiation, tracheary elements undergo PCD, which results in a continuous transport system of empty cells (Bollhöner et al., 2012). However, no evident defects in vascular tissues were detected in *A. thaliana* plants

growing in the presence of 1 µM Fer-1, indicating that vascular differentiation does not likely involve a ferroptotic type of cell death (Fig. S5 d).

Expression of cell death markers in plant cells after 55°C HS

As an initial approach to identify markers of ferroptotic plant cell death, we examined the expression pattern of 30 candidate genes in roots from plants exposed to 55°C HS ± Fer-1 (Table S1 and Table S2). As can be observed in Fig. 5 a, the death of root cells triggered by 55°C HS is prevented by Fer-1, as previously shown for root hairs. The genes tested were (a) asparagine synthetase genes *ASN1*, *ASN2*, and *ASN3*, as *ASN* has been identified as a candidate ferroptosis marker in tumor cells (Dixon et al., 2014); (b) genes encoding voltage-dependent channels located in the mitochondrial membrane, as they have been reported to be essential for erastin-induced ferroptosis in human cancer cells *VDAC1*, *VDAC2*, *VDAC3*, *VDAC4*, and *VDAC5* (Yagoda et al., 2007); (c) cation transport regulator (Chac)-like genes, also reported as ferroptosis markers in cancer cells (*CCL1*, *CCL2*, and *CCL3*; Dixon et al., 2014); (d) *BAXI-1*, *HRD1*, *SEL1*, *BiP1*, *BiP2*, *BiP3*, and *bZIP60*, encoding for *Arabidopsis* ER stress markers, as an ER-stress signature has been found in erastin-induced cell death (Dixon et al., 2014); (e) *PR2*, *PR5*, *ACS2*, *LSD*, and *WRKY33* (Zheng et al., 2006), implicated in the hypersensitive response; (f) *Arabidopsis* autophagy markers *ATG7*, *ATG8*, and *ATG9* (Kim et al., 2012); (g) the vacuolar cell death–related gene *VPE* (Hara-Nishimura et al., 2005); (h) metacaspase genes *MC1* and *MC2* (Coll et al., 2010); (i) *kiss of death* (*KOD*), a gene encoding for a 25-aa peptide that induces cell death in *A. thaliana* roots (Blanvillain et al., 2011); and (j) as a control, *RHD6* and *WER*, implicated in root development (Han et al., 2003; Coll et al., 2010; Hara-Nishimura and Hatsugai, 2011; Bruex et al., 2012; Robert et al., 2012). We analyzed the expression of these 30 genes 2 h after HS treatment and observed down-regulation of most genes, or slight up-regulation that was further enhanced by Fer-1 (e.g., *GPT2a*, *VDAC5*, and *VPE*). One exception was *KOD*, which was significantly up-regulated in a Fer-1–sensitive manner (17-fold; Fig. 5, b and c). Together with previous results showing that KOD is induced by heat stress and peroxide (Blanvillain et al., 2011), our results suggest that KOD might be acting downstream of GSH depletion and ROS accumulation in the cascade of events that lead to 55°C HS–induced ferroptotic-like cell death and could serve as a molecular marker, albeit nonspecific, for this process.

Ferroptosis inhibitors increase basal thermotolerance of *Arabidopsis* seedlings

Our results indicated that 55°C HS triggered ferroptosis-like cell death in plants. We next assessed the potential relevance of ferroptosis in vivo under more physiological conditions. Plants' inherent ability to tolerate high-temperature stress without prior conditioning is called basal thermotolerance. Basal thermotolerance is crucial, and together with acquired thermotolerance (acquired after acclimation), ultimately determines how well a plant copes with thermal changes in its environment. It has been shown that sudden HS induces the accumulation of ROS dependent on NOX activity (Wahid et al., 2007; Pucciariello et al., 2012). These data and our results with ferroptosis inhibitors suggest that plant cells might be dying in response to moderate HS via a NOX-dependent, ferroptosis-like pathway. Thus, ferroptosis inhibitors might ultimately find utility in the protection of crops during times of extreme temperature fluctuations, which is of increasing concern because of ongoing climate change. Thus, we assessed whether ferroptosis inhibitors could improve the ability of plants to cope with exposure to lethal temperatures at which many crops could be exposed in the environment. A temperature of 43°C was tested for 1 h, as when exposed to these conditions, plants without acclimation treatment collapse and bleach (Fig. 6; Meiri and Breiman, 2009). When plants were cotreated with Fer-1 or CPX, they showed a significantly increased ability to survive at this otherwise lethal temperature (Fig. 6). Although control plants submitted to a 43°C HS bleached in the course of 3 d, around 70% of the plants pretreated with CPX survived the treatment. The fraction of surviving plants was 30% when plants were pretreated with Fer-1. In addition, treatment with DPI also increased the rate of survival to 42% (Fig. 6). This result suggested that NOX activity was implicated in the pathway triggered by this treatment, meaning that oxidative stress might be a significant component of the heat-induced damage induced. Also, this shows that a similar process to the one observed in roots and cell suspensions in response to the 55°C HS is taking place in these plants.

Previous experiments in nonphotosynthetic tissues (roots and cell suspensions grown in the dark) showed that active chloroplasts are not essential for ferroptosis-like cell death. However, the aerial parts of plants exposed to 43°C were observed to die after HS, suggesting that chloroplasts might be involved in the cell death pathway triggered at this temperature in photosynthetic tissues. We tested this possibility by stressing the plants and maintaining them in the dark, before analysis. As shown in Fig. 6, seedlings kept in the dark died at lower rates than the ones exposed to the light, suggesting that active chloroplasts are contributing to cell death in leaves, either as a source of iron or as a source of ROS. This cell death was prevented when plants were preincubated with Fer-1 before 43°C HS. These results, obtained at temperatures that can be easily reached in the field, suggest that HS normally causes ferroptosis-like cell death in plants and that suppressing this death may be of practical value in agricultural applications.

Discussion

Ferroptosis was described in tumor cells as a cell death mechanism involving iron-dependent ROS accumulation. This process can be triggered by GSH depletion (Yang et al., 2014) and results in cell death that is morphologically distinct from other known forms of cell death such as apoptosis, necrosis, and autophagy (Dixon et al., 2012). The results presented here demonstrate that a similar form of iron-dependent, ferroptosis-like cell death also takes place in plant cells. In particular, our results suggest a physiological role for ferroptosis-like death in plant responses to environmental stress.

Many of the hallmarks that characterize ferroptosis in animal cells are conserved in plants exposed to heat stress. Notably, dying cells showed normal nuclei but shrunken mitochondria, an accumulation of intracellular ROS, and depletion of GSH and AA. Moreover, death was prevented by the canonical ferroptosis inhibitors Fer-1 and CPX. These results suggest that plant cells undergoing ferroptosis cannot overcome the ROS accumulation induced by HS. As the depletion of neither GSH nor AA is reverted back by cotreatment with ferroptosis

a

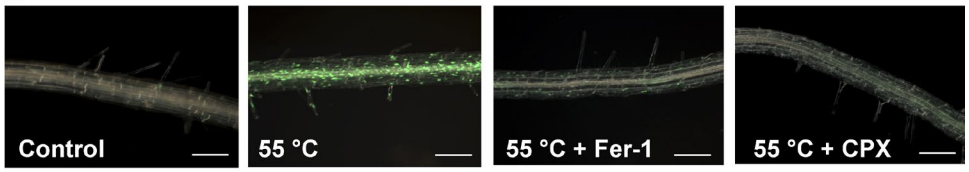

b

Category	Gene	55 ºC/D	55 ºC + Fer-1/D	55 ºC CPX/D	P value (one way ANOVA)
Arabidopsis genes with homology to ferroptosis markers	*ASN 1*	0.56 ± 0.11	0.12 ± 0.04	0.35 ± 0.37	0.1318
	ASN 2	0.37 ± 0.05	1.17 ± 0.19	n d	0.0021
	ASN 3	0.50 ± 0.10	1.42 ± 0.26	n d	0.0046
	CCL1	0.79 ± 0.18	0.99 ± 0.27	1.34 ± 0.53	0.2432
	CCL2	0.52 ± 0.04	0.46 ± 0.08	1.23 ± 0.22	0.0008
	CCL3	0.47 ± 0.08	2.21 ± 0.53	n d	0.0049
	GPT2a	1.18 ± 0.20	3.13 ± 0.58	1.11 ± 0.38	0.0016
	GPT2b	0.21 ± 0.06	0.46 ± 0.11	n d	0.0259
Voltage-dependent anion-selective channel	*VDAC1*	0.65 ± 0.30	1.42 ± 0.21	2.37 ± 0.43	0.0020
	VDAC2	1.29 ± 0.14	1.3 ± 0.15	2.46 ± 0.59	0.0111
	VDAC3	0.48 ± 0.24	1.24 ± 0.65	0.83 ± 0.35	0.1964
	VDAC4	0.41 ± 0.19	0.63 ± 0.32	0.72 ± 0.29	0.4130
	VDAC5	2.89 ± 0.80	4.21 ± 1.03	2.11 ± 0.75	0.0645
ER stress	*BAX-1*	0.72 ± 0.28	1.15 ± 0.49	0.88 ± 0.29	0.4047
	HRD1	0.83 ± 0.34	1.58 ± 0.66	1.20 ± 0.52	0.2884
	SEL-1	0.62 ± 0.09	1.09 ± 0.25	1.58 ± 1.22	0.3325
	BIP1	0.19 ± 0,02	0.25 ± 0.02	0.37 ± 0.02	0.0031
	BIP2	0.17 ± 0,01	0.25 ± 0.01	0.34 ± 0.01	0.0003
	BIP3	0.04 ± 0,01	0.04 ± 0.02	0.07 ± 0.01	0.1482
	BZIP60	0.13 ± 0,03	0.09 ± 0.01	0.27 ± 0.03	0.0131
Hypersensitive response cell death	*PR2*	n d	n d	n d	-
	PR5	n d	n d	n d	-
	WRKY33	0.12 ± 0.01	0.14 ± 0.01	0.34 ± 0.06	0.0005
	LSD1	0.82 ± 0.11	1.02 ± 0.22	1.99 ± 0.46	0.0066
	ACS2	0.94 ± 0.77	2.38 ± 1.71	4.06 ± 3.54	0.3241
Autophagy	*ATG7*	1.10 ± 0.26	1.95 ± 0.39	n d	0.0348
	ATG8	1.03 ± 0.16	1.24 ± 0.16	3.41 ± 2.27	0.1248
	ATG9	0.83 ± 0.16	1.00 ± 0.13	0.59 ± 0.21	0.0664
Vacuolar cell death	*VPE*	4.18 ± 1.5	10.63 ± 4.43	n d	0.0753
Metacaspases	*MC1*	1.12 ± 0.39	2.53 ± 0.77	2.73 ± 1.38	0.1525
	MC2	0.31 ± 0.11	0.11 ± 0.03	n d	0.0385
Kiss of Death	*KOD*	17.44 ± 4.76	6.59 ± 0.86	nd	0.0178
Root development (control)	*RHD6*	0.53 ± 0.1	0.38 ± 0.20	0.86 ± 0.32	0.0956
	WER	0.79 ± 0.20	1.56 ± 0.38	4.68 ± 3.23	0.0940

c

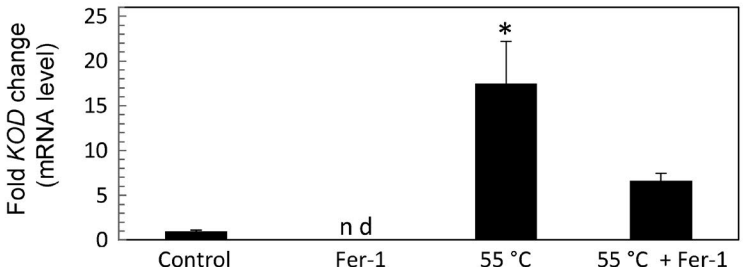

Figure 5. **Expression of candidate *Arabidopsis* ferroptosis marker genes.** (a) *Arabidopsis* roots from 6-d-old seedlings were preincubated with 1 µM Fer-1, 10 µM CPX, or DMSO (control). Cell death was induced by treating roots at 55°C for 10 min, and roots were stained with Sytox green 6 h after treatment. The images show that cells in the main root undergo cell death that is prevented by ferroptosis inhibitors. Bars, 50 µm. (b) Changes in expression of candidate genes that might be associated with plant ferroptosis in *A. thaliana* roots 2 h after HS at 55°C for 10 min. mRNA levels are expressed as a fold-change ratio between the different conditions and were analyzed by one-way analysis of variance (ANOVA). D, DMSO; nd, not determined. (c) mRNA expression levels of KOD determined by real-time quantitative PCR in *A. thaliana* roots in response to 55°C for 2 h. Data are from three independent biological replicates and presented as mean ± SD. Data were analyzed by one-way analysis of variance. *, $P < 0.05$. Significance is indicated relative to the treatment at 55°C plus the ferroptosis inhibitor Fer-1.

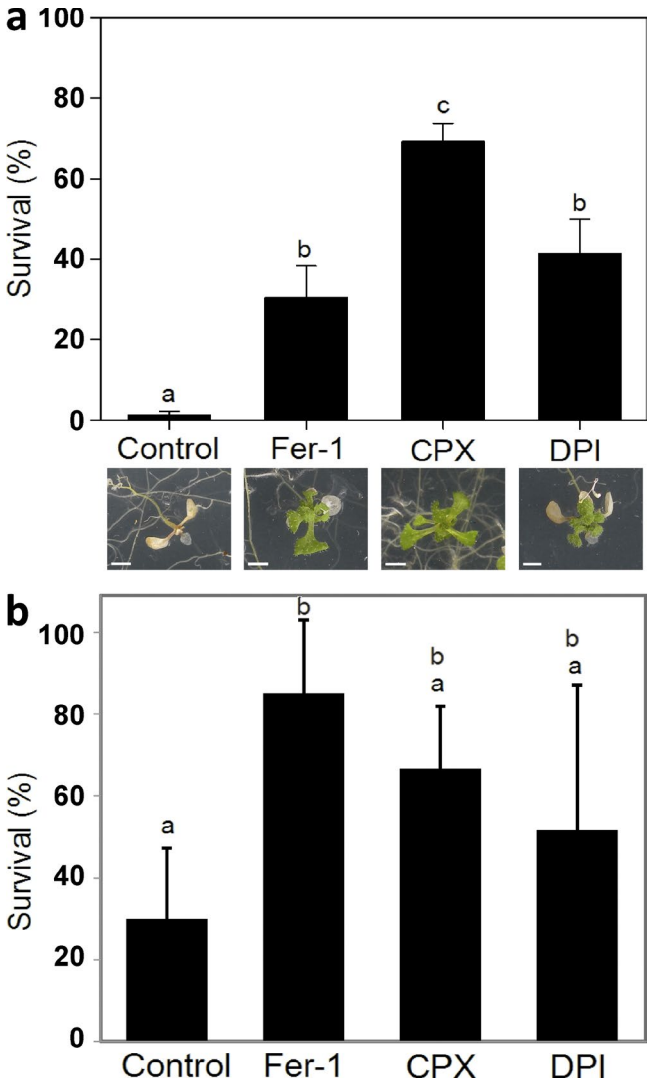

Figure 6. **Ferroptosis inhibitors and DPI increase the rate of thermotolerance in *Arabidopsis* seedlings.** (a) *A. thaliana* seedlings were grown on agar plates at 22°C for 6 d. Plates were pretreated as indicated for 16 h, exposed to HS (43°C for 1 h), and then returned to 22°C. The survival rate was determined 5 d after HS. Bottom panels show a representative picture of each case. Bars, 50 mm. (b) *A. thaliana* seedlings were grown on agar plates at 22°C for 6 d. Plates were pretreated as indicated in the dark for 16 h, exposed to HS (43°C for 1 h), and then returned to 22°C, avoiding exposure to light. The survival rate was determined 7 d after HS. (a and b) Control plates were pretreated with 1:1,000 DMSO. Each value is the mean ± SEM of at least 15 independent experiments. For each experiment, 20 seedlings per plate were tested. Different letters denote statistical difference (one-way analysis of variance, $P < 0.05$).

inhibitors, depletion of GSH and reduced AA may be an early event, probably before ROS accumulation through NOX activity and lipid peroxidation, as observed in tumor cells (Dixon et al., 2012; Yang et al., 2014). The mechanisms through which GSH is depleted in plant cells are not yet well understood. However, because of accumulation of unfolded proteins in the ER during heat stress (Yang et al., 2016b), more GSH might be consumed to reduce incorrectly formed disulfide bonds (Ozgur et al., 2014). This, together with the unfolding and inhibition of GSH biosynthetic enzymes, might explain GSH depletion and ROS accumulation in plant cells exposed to HS. Additionally, the low levels of reduced AA detected after HS might be caused by a failure in AA recycling attributable to the drop in GSH levels (Foyer and Noctor, 2011). In addition to soluble ROS via NOX activity, ferroptosis involves the accumulation of lipid ROS, which are typically formed through peroxidation of PUFA chains of membrane lipids (Skouta et al., 2014). The requirement of PUFA peroxidation for ferroptosis was recently reported in human cells by the use of PUFAs containing the heavy hydrogen isotope deuterium at the site of peroxidation (Yang et al., 2016a), which prevented PUFA oxidation and blocked ferroptosis. A similar result was obtained in *Arabidopsis* root hairs, where pretreatment with D-PUFAs protect root hairs exposed to a 55°C HS, preventing cell death (Fig. 3 e).

The study of the expression pattern of several genes related to cell death processes in plants or tumor cells showed that a recently described gene, *KOD*, which encodes a short peptide that regulates plant PCD, seems to be specifically regulated in *Arabidopsis* ferroptosis-like cell death (Blanvillain et al., 2011). Not only was *KOD* up-regulated after HS, but it was also induced in a ferroptosis-dependent manner (Fig. 5). This small peptide was shown previously to be induced by heat stress and peroxide (Blanvillain et al., 2011), which indicates that KOD might be acting downstream of GSH and AA depletion in the cascade of events that lead to cell death after HS in *Arabidopsis*. As Fer-1 is not able to prevent cell death induced directly by peroxide, but *KOD* has been shown to be induced upon peroxide application (Blanvillain et al., 2011), these results together suggest that the iron-dependent pathway shown herein might merge with the peroxide-induced pathway in which KOD was previously reported to act. The ability of Fer-1 to suppress KOD up-regulation suggests that ROS accumulation, downstream of GSH depletion, is an essential signal regulating KOD expression. Additionally, calcium efflux from the ER has been suggested to act downstream KOD. Thus, KOD may regulate calcium mobilization, which is in agreement with the requirement of calcium that we found for plant ferroptosis-like cell death (Fig. 1 b). Concordantly, a calcium requirement was also shown in a recently described form of oxidative cell death in mouse cells that appears to be related to ferroptosis (oxytosis). In oxytosis, calcium influx is observed downstream of GSH depletion and ROS accumulation (Henke et al., 2013). In summary, KOD is a candidate molecular marker of ferroptosis-like cell death in plants.

Fluctuations in environmental conditions occur naturally during plant development and reproduction. Extreme variations in temperature during hot summers are already known to cause significant agricultural yield losses (Bita and Gerats, 2013). Here we find that inhibitors of ferroptosis prevent the death of plants exposed to otherwise lethal temperatures. Importantly, the temperatures used in our thermotolerance experiments are conditions that can be reached in the field (HanumanthaRao et al., 2016). This finding indicates that the death of plants exposed to these lethal temperatures could involve a ferroptotic-like pathway. This may suggest new ways to protect crops during times of extreme temperature fluctuations, which is crucial as more extreme temperature events are expected with the ongoing climate change. Notably, a connection between HS and ferroptosis was also recently found in cancer cells (Sun et al., 2015). HSPB1 (also called mouse HSP25 or human HSP27), a member of the family of the small HS proteins (HSPs), is strongly induced after treatment with the ferroptosis trigger erastin in cancer cells, and the phosphorylated form of HSPB1 acts as a negative regulator of ferroptosis by

inhibiting cellular iron uptake and lipid ROS production (Sun et al., 2015). In *Caenorhabditis elegans*, HS triggers a regulated form of cell death that was described as a regulated necrosis that involves calcium and the expression of HSPs (Kourtis et al., 2012). Overexpression of HSF-1, a transcription factor that regulates the expression of HSPs, suppresses HS-induced cell death in *C. elegans*. Notably, members of class A HSFs, including *Arabidopsis* HSF-1 and -3, play a fundamental role in regulating the HS response in plants. Furthermore, it was recently reported that overexpression of a constitutively active form of A-HSF1 caused the induction of many HSP genes and improved the thermotolerance of plants (Ohama et al., 2016), suggesting that similar pathways might be triggered in response to HS in plant and animal systems.

In conclusion, an iron-dependent, oxidative cell death process with biochemical and morphological similarities to ferroptosis, as described in mammalian cells, has a physiological role in plants, regulating plant cell death in response to heat stress. Although additional factors involved in this ferroptosis-like pathway remain to be identified in plants, many characteristics are conserved between plants and animal cells. These results not only suggest that ferroptosis might be a conserved form of cell death, but also raise interesting evolutionary questions. Ferroptosis might be an ancient form of cell death or the result of convergent evolution in plants. Either way, this iron-dependent oxidative form of cell death represents a common solution across kingdoms, whose evolutionary basis can be the subject of future studies.

Materials and methods

Cell suspension culture growth

Cell suspension cultures of *A. thaliana* were grown essentially as previously described (May and Leaver, 1993). In brief, cultures were grown in 50 ml of liquid Murashige and Skoog medium (basal salts 4.3 g/l) containing 0.5 mg/l 1-naphthylacetic acid (NAA), 0.05 mg/l kinetin, and 3% (wt/vol) sucrose, pH 5.8, with agitation on an orbital shaker (100 rpm) under dark conditions in a controlled environment room at 23°C. Cultures were subcultured every 7 d into fresh medium.

Plant growth conditions

A. thaliana (Col-O) seeds were sterilized in 50% ETOH for 1 min and then 10 min in a bleach-SDS solution (50% bleach and 1% SDS), followed by extensive washing with sterile distilled water.

After sterilization, all seeds were plated in a single line on ATS growing medium to allow the roots to grow down the surface and stratified at 4°C for 48 h, before being placed vertically at 23°C, 16 h light, 8 h dark (Estelle and Somerville, 1987).

Heat treatment of cell suspension cultures

10 ml of a 7-d-old cell culture pretreated according each experiment was placed in sterile 50-ml flasks and treated with the indicated temperature in a water bath with shaking (85 oscillations/min). After heat treatment, flasks were returned to the controlled environment room, with shaking, until scoring 24 h later.

Treatments of roots

6-d-old seedlings were pretreated with the indicated solutions in a 1.5-ml tube in a controlled environment room. Heat treatments were performed in sterile distilled water, placing pretreated 6-d-old seedlings in a water bath at the indicated temperature without shaking for 10 min. After HS, the seedlings were returned to a controlled environment room at a constant temperature of 23°C in the light for the indicated times, after which cell death was scored.

Fer-1, CPX, DPI, Nec-1, CHO, and D-PUFAs (Retrotope) were applied to *Arabidopsis* roots 16 h before the HS treatment. For H_2O_2 treatments, seedlings were pretreated with or without Fer-1 in a 1.5-ml tube in a controlled environment room for 16 h. Seedlings were then treated with 150 mM H_2O_2 for 6 h. For NaCl treatments, seedlings were pretreated with or without Fer-1 in a 1.5-ml tube in a controlled environment room for 2 h, and then treated with 150 mM NaCl for 16 h. To study the optimal concentration to determine the effect of NaCl, three different concentrations of NaCl (50, 80, and 150 mM) were tested, and cell morphology was observed by DIC microscopy, to avoid a concentration that triggers a necrotic cell death response. Cell death after the three treatments was observed at similar rates, and for the three concentrations tested, cell death was not prevented with Fer-1 or with CPX. In addition, root hairs showed only partial retraction of cytoplasm, which appeared highly granulated for all three concentrations tested (a representative photo is shown in Fig. 2). The morphology observed was not necrotic. For the case of H_2O_2 treatments, ROS in root cells was assayed before treatments to ensure that plants were not undergoing oxidative stress. To adjust the experiment, different concentrations of H_2O_2 were tested (1, 25, 30, and 150 mM) with and without the addition of ferroptosis inhibitors. Whereas 1 mM was not enough to trigger cell death in root hairs, 15 mM H_2O_2 induced 40% of cell death, 25 mM and 30 mM induced ∼55%, and 150 mM induced cell death ∼65%. In all cases, the morphology of the root hairs was not necrotic; a representative picture is shown in Fig. 2.

For calcium requirement studies, 6-d-old seedlings were preincubated with 3 mM $CaCl_2$ for 16 h, 1 mM EGTA for 2 h, or EGTA for 2 h and then with 3 mM $CaCl_2$ for 16 h before inducing cell death by treating roots at 55°C for 10 min as explained earlier. 200 µM Fe-Na-EDTA, 5 µM $CuSO_4$, 3 mM Cl_2Mn, and 3 mM Cl_2Mg were applied for 16 h before inducing cell death by treating roots at 55°C for 10 min as explained earlier. For all treatments, root hairs were stained with Sytox green, and dead and living root hairs were quantified.

Cell death quantification

Cells/roots were stained with Sytox green, a nucleic acid stain that easily penetrates cells with compromised plasma membranes. Root hairs/cells were stained in a 1-µg/ml solution of Sytox green for 10 min. After incubation, root hairs were washed with 20 mM Hepes buffer, pH 7.2 (buffer A), and immediately quantified using confocal microscopy (Eclipse C1 Plus Confocal microscope using EZ-C1 3.80 imaging software and Ti-Control; Nikon). All images were taken at RT using buffer A as the medium with a CFI Super Fluor 40× oil lens (NA 1.3; Nikon). Roots were imaged using 15% laser power and a small pinhole. Images were organized using Photoshop CC (Adobe Systems). Cell death in cell suspensions was quantified by using a fluorometer (Fluoroscan II).

Analysis and imaging of ROS production

H_2DCFDA was prepared as a 10 mM stock solution in DMSO and frozen at −20°C. MitoSOX red was prepared fresh at a 5 mM concentrated solution in DMSO for each use. C11-BODIPY$^{581/591}$ was prepared at 2 mM in DMSO. H_2DCFDA, mitoSOX red, and C11-BODIPY$^{581/591}$ were purchased from Molecular Probes. Stock solutions were diluted 1:1,000 in buffer A in each experiment.

Cell cultures and 6-d-old plants were incubated for 10 min at RT with the working solution containing the dyes, in 12- or 24-well plates. After incubation, cells were washed with buffer A and immediately scored using a Fluoroscan. Roots were washed with buffer A and immediately

quantified using confocal microscopy (Eclipse C1 Plus Confocal microscope using EZ-C1 3.80 imaging software and Ti-Control). All images were taken at RT using buffer A as the medium with a CFI Super Fluor 40× oil lens (NA 1.3). Roots were imaged using 15% laser power and a small pinhole. Images were organized using Photoshop CC.

TEM analysis

Seedlings grown vertically for 6 d on ATS plates and subjected to the indicated treatments were fixed using 2.5% (vol/vol) glutaraldehyde in PBS buffer overnight at 4°C. In parallel, a fraction of the seedlings were not fixed and were stained with Sytox green to score for cell death in cortical cells. Cells from roots submitted to heat stress showed Sytox green staining in cortical cells as shown in Videos 1, 2, 3, and 4. After washing three times in PBS buffer, the specimens were postfixed with 1% (vol/vol) osmium tetroxide in the medium buffer for 1 h and washed twice in distilled water. Samples were dehydrated with 50%, 70%, 95%, and 100% ethanol and infiltrated and embedded in Spurr's resin. Roots were sectioned from the tip upward using a glass knife on an EM UC7 ultramicrotome (Leica Biosystems). Roots were continuously oriented transversely to the root axis to allow recording of the distance from the root tip by counting sections. Ultrathin (80-nm) sections were made using a Diatome diamond knife on an EM UC7, collected onto copper grids, and treated with 5% uranyl acetate in water for 60 min followed by Sato's lead staining for 5 min. Sections were examined in a transmission electron microscope (1230; Jeol). Digital images were captured using a Gatan MSC 600CW.

Effect of ferroptosis inhibitors on reproductive and vascular development

We examined buds and pistils composing the inflorescence ranging in size between 1 and 8 mm, looking for two key events involving cell death: megaspore cell death and synergid cell death. To test the effect of Fer-1 and CPX on reproductive development, *Arabidopsis* inflorescences were dipped for three consecutive days in a work solution containing either 10 µM CPX or 1 µM Fer-1 (in 0.1% DMSO and 0.01% Silwet L-77) or in a mock solution (0.1% DMSO and 0.01% Silwet L-77). For each treatment, five plants were treated, and a minimum of three inflorescences per plant were used for studies. Analysis of the treated inflorescences started on day 4. To analyze the buds in which we were expecting to find only a functional megaspore inside the ovules as a result of megaspore death, 1–1.25-mm pistils were selected. Embryo sacs were evaluated by DIC microscopy. To analyze whether synergid cell death was compromised, which would lead to fertilization problems, the ratio of fertilized to unfertilized embryo sacs was analyzed in self-pollinated flowers after treatment. To perform this experiment, we selected those flowers exposed to the treatments that showed signs of pollination (pollen on the stigma) at day 3. At day 4, the pistils were dissected, and fertilization was assessed by DIC microscopy.

RNA isolation and quantitative real-time RT-PCR

Total RNA from leaves and roots was extracted using TRIzol reagent (Invitrogen) according to the manufacturer's recommendations, and samples were treated with RQ1 RNase-free DNase (Promega) to remove DNA contamination. For cDNA synthesis, 1 µg of total RNA was reverse transcribed by IMPROM II (Thermo Fisher Scientific) using random primers (Biodynamics). Real-time PCRs were performed in a Step One real-time PCR system (Applied Biosystems) using SYBR green PCR master mix (Applied Biosystems) as described by the manufacturer. The cycling program was 40 cycles at 95°C for 10 min and 1 min at 60°C; a melting curve analysis was performed at the end of the PCR. Primer pairs were tested for specificity and for amplification efficiency with a standard cDNA dilution curve. The different biological samples were subsequently normalized against expression of *UBQ5*, encoding a ubiquitin gene. Quantitative expression analysis was conducted for at least three independent experiments including at least three independent biological replicates per sample in each experiment.

Thermotolerance testing

6-d-old seedlings growing at 22°C were exposed to 43°C for 1 h and then allowed to recover at 22°C for 5 d. Those seedlings that were still green and continued to produce new leaves were scored as survivors. Experiments were performed after pretreating the seedlings on a plate with 1:1,000 DMSO (control plates) or with 1 µM Fer-1 or 10 µM CPX for 16 h. Control plates exhibited a survival rate <10%.

GSH and AA quantification

Roots were harvested (~400 mg) and powdered with liquid N_2, and AA and GSH were extracted and determined as previously reported (Griffith, 1980; Bartoli et al., 2006, respectively). Concentrations of both AA and GSH obtained in control seedlings root were as previously described for plants grew under similar conditions (Ramírez et al., 2013).

TUNEL assay

6-d-old seedlings were submitted to heat treatments at the indicated temperature for 10 min. After HS, the seedlings were returned to a controlled environment room at a constant temperature of 23°C in the light for 6 h. Then, TUNEL assays were performed with the Click-iT TUNEL Alexa Fluor imaging kit (Thermo Fisher Scientific) according to the manufacturer's instructions.

Mitochondrial area quantification

Roots of 6-d-old seedlings were stained with MitoTracker green FM (200 nM; Molecular Probes) for 45 min. Mitochondrial images were obtained using confocal microscopy (Eclipse C1 Plus Confocal microscope using EZ-C1 3.80 imaging software and Ti-Control) at different times (0, 1, 3, and 6 h after HS). Automated quantification of mitochondrial area was performed using the Mito-Morphology macro for ImageJ software (version 1.39; National Institutes of Health) as described previously (Dagda et al., 2009). In brief, the green channel of cells stained with MitoTracker green FM was converted to grayscale and inverted (to show mitochondria-specific fluorescence as black pixels), and the threshold was set to optimally resolve individual mitochondria. The macro traces mitochondrial outlines using the command "analyze particles."

Sequence comparison

Sequence similarity searches were performed on the National Center for Biotechnology Information website using protein–protein BLAST programs against the *A. thaliana* database.

Online supplemental material

Fig. S1 shows the effect of the necroptosis inhibitor Nec-1 and divalent transition metal ions on cell death induced by a 55°C HS treatment. Fig. S2 shows that 55°C HS in *Arabidopsis* cell suspensions triggers the accumulation of ROS, which can be inhibited by Fer-1, CPX, and DPI. Fig. S3 shows that mitoSOX is not involved in the cell death triggered by a 55°C treatment in *Arabidopsis* root hairs. Fig. S4 shows that caspase-like activity is required for cell death after 55°C HS, but DNA fragmentation is not detected. Fig. S5 shows the effect of ferroptosis inhibitors on reproductive and vascular development in *A. thaliana*. Table S1 shows the identity of the transcriptional pharmacodynamic ferroptosis markers reported in Dixon et al. (2014) and putative orthologues found in *A. thaliana.* Table S2 lists the primer pairs used for quantitative PCR. Videos 1, 2, 3, and 4 show Sytox green staining of the different cell types that compose the root after a 55°C HS treatment.

Acknowledgments

We thank Mikhail S. Shchepinov for providing D-PUFAs, Monica Kotler for providing Nec-1, and Maria Ana Contin for providing Ac-DEVD-CHO. We thank Daniela Villamonte for technical assistance with confocal microscopy.

This research was funded by grants to G.C. Pagnussat from Agencia Nacional de Promoción Científica y Técnica Argentina (PICT 1809) and from the Howard Hughes Medical Institute (International Early Career Scientist award 55007430); grants to B.R. Stockwell from the National Institutes of Health (5R01CA097061 and R35CA209896); R00 Award to S.J. Dixon from the National Cancer Institute (4R00CA166517-03); and a grant to D.F. Fiol from Agencia Nacional de Promoción Científica y Técnica Argentina (PICT 1524). A.M. Distéfano and S. D'Ippólito are postdoctoral fellows of Consejo Nacional de Investigaciones Científicas y Técnicas (CONICET); J.P. Córdoba, A.M. Bellido, and D. Soto are graduate fellows of CONICET. M.V. Martin, C.G. Bartoli, E.J. Zabaleta, D.F. Fiol, and G.C. Pagnussat are CONICET researchers.

The authors declare no competing financial interests.

Author contributions: Conceptualization, G.C. Pagnussat, S.J. Dixon, B.R. Stockwell, D.F. Fiol, E.J. Zabaleta, M.V. Martin, and A.M. Distéfano; methodology, G.C. Pagnussat, S.J. Dixon, B.R. Stockwell, D.F. Fiol, M.V. Martin, and A.M. Distéfano; investigation; M.V. Martin, A.M. Distéfano, G.C. Pagnussat, J.P. Córdoba, J.A. Roldán, A.M. Bellido, S. D'Ippólito, S.L. Colman, D. Soto, and C.G. Bartoli; formal analysis, M.V. Martin, A.M. Distéfano, and D.F. Fiol; supervision, G.C. Pagnussat, S.J. Dixon, B.R. Stockwell, and D.F. Fiol; and writing of the original draft, G.C. Pagnussat, S.J. Dixon, B.R. Stockwell, D.F. Fiol, M.V. Martin, and A.M. Distéfano.

Submitted: 27 May 2016
Revised: 29 September 2016
Accepted: 7 December 2016

References

Bartoli, C.G., J. Yu, F. Gómez, L. Fernández, L. McIntosh, and C.H. Foyer. 2006. Inter-relationships between light and respiration in the control of ascorbic acid synthesis and accumulation in *Arabidopsis* thaliana leaves. *J. Exp. Bot.* 57:1621–1631. http://dx.doi.org/10.1093/jxb/erl005

Bergsbaken, T., S.L. Fink, and B.T. Cookson. 2009. Pyroptosis: Host cell death and inflammation. *Nat. Rev. Microbiol.* 7:99–109. http://dx.doi.org/10.1038/nrmicro2070

Bita, C.E., and T. Gerats. 2013. Plant tolerance to high temperature in a changing environment: Scientific fundamentals and production of heat stress-tolerant crops. *Front. Plant Sci.* 4:273. http://dx.doi.org/10.3389/fpls.2013.00273

Blanvillain, R., B. Young, Y.M. Cai, V. Hecht, F. Varoquaux, V. Delorme, J.-M. Lancelin, M. Delseny, and P. Gallois. 2011. The *Arabidopsis* peptide kiss of death is an inducer of programmed cell death. *EMBO J.* 30:1173–1183. http://dx.doi.org/10.1038/emboj.2011.14

Bollhöner, B., J. Prestele, and H. Tuominen. 2012. Xylem cell death: Emerging understanding of regulation and function. *J. Exp. Bot.* 63:1081–1094. http://dx.doi.org/10.1093/jxb/err438

Bruex, A., R.M. Kainkaryam, Y. Wieckowski, Y.H. Kang, C. Bernhardt, Y. Xia, X. Zheng, J.Y. Wang, M.M. Lee, P. Benfey, et al. 2012. A gene regulatory network for root epidermis cell differentiation in *Arabidopsis*. *PLoS Genet.* 8:e1002446. http://dx.doi.org/10.1371/journal.pgen.1002446

Choi, C.Q. 2013. The fate of the plant embryo's suspensor: Balancing life and death. *PLoS Biol.* 11:e1001656. http://dx.doi.org/10.1371/journal.pbio.1001656

Christensen, C.A., S.W. Gorsich, R.H. Brown, L.G. Jones, J. Brown, J.M. Shaw, and G.N. Drews. 2002. Mitochondrial GFA2 is required for synergid cell death in *Arabidopsis*. *Plant Cell.* 14:2215–2232. http://dx.doi.org/10.1105/tpc.002170

Christofferson, D.E., and J. Yuan. 2010. Necroptosis as an alternative form of programmed cell death. *Curr. Opin. Cell Biol.* 22:263–268. http://dx.doi.org/10.1016/j.ceb.2009.12.003

Coll, N.S., D. Vercammen, A. Smidler, C. Clover, F. Van Breusegem, J.L. Dangl, and P. Epple. 2010. *Arabidopsis* type I metacaspases control cell death. *Science.* 330:1393–1397. http://dx.doi.org/10.1126/science.1194980

Courtois-Moreau, C.L., E. Pesquet, A. Sjödin, L. Muñiz, B. Bollhöner, M. Kaneda, L. Samuels, S. Jansson, and H. Tuominen. 2009. A unique program for cell death in xylem fibers of *Populus* stem. *Plant J.* 58:260–274. http://dx.doi.org/10.1111/j.1365-313X.2008.03777.x

Dagda, R.K., S.J. Cherra III, S.M. Kulich, A. Tandon, D. Park, and C.T. Chu. 2009. Loss of PINK1 function promotes mitophagy through effects on oxidative stress and mitochondrial fission. *J. Biol. Chem.* 284:13843–13855. http://dx.doi.org/10.1074/jbc.M808515200

Danon, A., V.I. Rotari, A. Gordon, N. Mailhac, and P. Gallois. 2004. Ultraviolet-C overexposure induces programmed cell death in *Arabidopsis*, which is mediated by caspase-like activities and which can be suppressed by caspase inhibitors, p35 and Defender against Apoptotic Death. *J. Biol. Chem.* 279:779–787. http://dx.doi.org/10.1074/jbc.M304468200

Dixon, S.J., K.M. Lemberg, M.R. Lamprecht, R. Skouta, E.M. Zaitsev, C.E. Gleason, D.N. Patel, A.J. Bauer, A.M. Cantley, W.S. Yang, et al. 2012. Ferroptosis: An iron-dependent form of nonapoptotic cell death. *Cell.* 149:1060–1072. http://dx.doi.org/10.1016/j.cell.2012.03.042

Dixon, S.J., D.N. Patel, M. Welsch, R. Skouta, E.D. Lee, M. Hayano, A.G. Thomas, C.E. Gleason, N.P. Tatonetti, B.S. Slusher, and B.R. Stockwell. 2014. Pharmacological inhibition of cystine-glutamate exchange induces endoplasmic reticulum stress and ferroptosis. *eLife.* 3:e02523. http://dx.doi.org/10.7554/eLife.02523

Drew, M.C., C.-J. He, and P.W. Morgan. 2000. Programmed cell death and aerenchyma formation in roots. *Trends Plant Sci.* 5:123–127. http://dx.doi.org/10.1016/S1360-1385(00)01570-3

Drews, G.N., and A.M. Koltunow. 2011. The female gametophyte. *Arabidopsis Book.* 9:e0155. http://dx.doi.org/10.1199/tab.0155

Estelle, M., and C. Somerville. 1987. Auxin-resistant mutants of *Arabidopsis thaliana* with an altered morphology. *Mol. Gen. Genet.* 206:200–206. http://dx.doi.org/10.1007/BF00333575

Foyer, C.H., and G. Noctor. 2011. Ascorbate and glutathione: The heart of the redox hub. *Plant Physiol.* 155:2–18. http://dx.doi.org/10.1104/pp.110.167569

Franco, R., and J.A. Cidlowski. 2012. Glutathione efflux and cell death. *Antioxid. Redox Signal.* 17:1694–1713. http://dx.doi.org/10.1089/ars.2012.4553

Friedmann Angeli, J.P., M. Schneider, B. Proneth, Y.Y. Tyurina, V.A. Tyurin, V.J. Hammond, N. Herbach, M. Aichler, A. Walch, E. Eggenhofer, et al. 2014. Inactivation of the ferroptosis regulator Gpx4 triggers acute renal failure in mice. *Nat. Cell Biol.* 16:1180–1191. http://dx.doi.org/10.1038/ncb3064

Ge, Y., Y.M. Cai, L. Bonneau, V. Rotari, A. Danon, E.A. McKenzie, H. McLellan, L. Mach, and P. Gallois. 2016. Inhibition of cathepsin B by caspase-3 inhibitors blocks programmed cell death in *Arabidopsis*. *Cell Death Differ.* 23:1493–1501. http://dx.doi.org/10.1038/cdd.2016.34

Griffith, O.W. 1980. Determination of glutathione and glutathione disulfide using glutathione reductase and 2-vinylpyridine. *Anal. Biochem.* 106:207–212. http://dx.doi.org/10.1016/0003-2697(80)90139-6

Gunawardena, A.H.L.A.N. 2008. Programmed cell death and tissue remodelling in plants. *J. Exp. Bot.* 59:445–451. http://dx.doi.org/10.1093/jxb/erm189

Gunawardena, A.H.L.A.N., J.S. Greenwood, and N.G. Dengler. 2004. Programmed cell death remodels lace plant leaf shape during development. *Plant Cell.* 16:60–73. http://dx.doi.org/10.1105/tpc.016188

Hakem, R., A. Hakem, G.S. Duncan, J.T. Henderson, M. Woo, M.S. Soengas, A. Elia, J.L. de la Pompa, D. Kagi, W. Khoo, et al. 1998. Differential requirement for caspase 9 in apoptotic pathways in vivo. *Cell.* 94:339–352. http://dx.doi.org/10.1016/S0092-8674(00)81477-4

Han, D., F. Antunes, R. Canali, D. Rettori, and E. Cadenas. 2003. Voltage-dependent anion channels control the release of the superoxide anion from mitochondria to cytosol. *J. Biol. Chem.* 278:5557–5563. http://dx.doi.org/10.1074/jbc.M210269200

HanumanthaRao, B., R.M. Nair, and H. Nayyar. 2016. Salinity and high temperature tolerance in mungbean [*Vigna radiata (L.) Wilczek*] from a physiological perspective. *Front. Plant Sci.* 7:957. http://dx.doi.org/10.3389/fpls.2016.00957

Hara-Nishimura, I., and N. Hatsugai. 2011. The role of vacuole in plant cell death. *Cell Death Differ.* 18:1298–1304. http://dx.doi.org/10.1038/cdd.2011.70

Hara-Nishimura, I., N. Hatsugai, S. Nakaune, M. Kuroyanagi, and M. Nishimura. 2005. Vacuolar processing enzyme: An executor of plant cell death. *Curr. Opin. Plant Biol.* 8:404–408. http://dx.doi.org/10.1016/j.pbi.2005.05.016

Henke, N., P. Albrecht, I. Bouchachia, M. Ryazantseva, K. Knoll, J. Lewerenz, E. Kaznacheyeva, P. Maher, and A. Methner. 2013. The plasma membrane channel ORAI1 mediates detrimental calcium influx caused by endogenous oxidative stress. *Cell Death Dis.* 4:e470. http://dx.doi.org/10.1038/cddis.2012.216

Hogg, B.V., J. Kacprzyk, E.M. Molony, C. O'Reilly, T.F. Gallagher, P. Gallois, and P.F. McCabe. 2011. An in vivo root hair assay for determining rates of apoptotic-like programmed cell death in plants. *Plant Methods.* 7:45. http://dx.doi.org/10.1186/1746-4811-7-45

Jamai, A., R. Tommasini, E. Martinoia, and S. Delrot. 1996. Characterization of glutathione uptake in broad bean leaf protoplasts. *Plant Physiol.* 111:1145–1152. http://dx.doi.org/10.1104/pp.111.4.1145

Jones, A.M. 2001. Programmed cell death in development and defense. *Plant Physiol.* 125:94–97. http://dx.doi.org/10.1104/pp.125.1.94

Kariya, K., T. Demiral, T. Sasaki, Y. Tsuchiya, I. Turkan, T. Sano, S. Hasezawa, and Y. Yamamoto. 2013. A novel mechanism of aluminum-induced cell death involving vacuolar processing enzyme and vacuolar collapse in tobacco cell line BY-2. *J. Inorg. Biochem.* 128:196–201. http://dx.doi.org/10.1016/j.jinorgbio.2013.07.001

Kim, S.-H., C. Kwon, J.-H. Lee, and T. Chung. 2012. Genes for plant autophagy: Functions and interactions. *Mol. Cells.* 34:413–423. http://dx.doi.org/10.1007/s10059-012-0098-y

Kourtis, N., V. Nikoletopoulou, and N. Tavernarakis. 2012. Small heat-shock proteins protect from heat-stroke-associated neurodegeneration. *Nature.* 490:213–218. http://dx.doi.org/10.1038/nature11417

Kranner, I., S. Birtić, K.M. Anderson, and H.W. Pritchard. 2006. Glutathione half-cell reduction potential: A universal stress marker and modulator of programmed cell death? *Free Radic. Biol. Med.* 40:2155–2165. http://dx.doi.org/10.1016/j.freeradbiomed.2006.02.013

Kroemer, G., L. Galluzzi, P. Vandenabeele, J. Abrams, E.S. Alnemri, E.H. Baehrecke, M.V. Blagosklonny, W.S. El-Deiry, P. Golstein, D.R. Green, et al. Nomenclature Committee on Cell Death 2009. 2009. Classification of cell death: Recommendations of the Nomenclature Committee on Cell Death 2009. *Cell Death Differ.* 16:3–11. http://dx.doi.org/10.1038/cdd.2008.150

Kuriki, T., T. Tsujiyama, N. Suzuki, and N. Suzuki. 1975. Spectrophotometric determination of iron(III) with ciclopirox olamine. *Bunseki Kagaku.* 24:112–115. http://dx.doi.org/10.2116/bunsekikagaku.24.112

Kwon, S.I., H.J. Cho, J.H. Jung, K. Yoshimoto, K. Shirasu, and O.K. Park. 2010. The Rab GTPase RabG3b functions in autophagy and contributes to tracheary element differentiation in *Arabidopsis*. *Plant J.* 64:151–164. http://dx.doi.org/10.1111/j.1365-313X.2010.04315.x

Linden, T., D.M. Katschinski, K. Eckhardt, A. Scheid, H. Pagel, and R.H. Wenger. 2003. The antimycotic ciclopirox olamine induces HIF-1alpha stability, VEGF expression, and angiogenesis. *FASEB J.* 17:761–763.

Lindsten, T., A.J. Ross, A. King, W.X. Zong, J.C. Rathmell, H.A. Shiels, E. Ulrich, K.G. Waymire, P. Mahar, K. Frauwirth, et al. 2000. The combined functions of proapoptotic Bcl-2 family members bak and bax are essential for normal development of multiple tissues. *Mol. Cell.* 6:1389–1399. http://dx.doi.org/10.1016/S1097-2765(00)00136-2

Linkermann, A., R. Skouta, N. Himmerkus, S.R. Mulay, C. Dewitz, F. De Zen, A. Prokai, G. Zuchtriegel, F. Krombach, P.-S. Welz, et al. 2014. Synchronized renal tubular cell death involves ferroptosis. *Proc. Natl. Acad. Sci. USA.* 111:16836–16841. http://dx.doi.org/10.1073/pnas.1415518111

Liu, Y., Y. Xiong, and D.C. Bassham. 2009. Autophagy is required for tolerance of drought and salt stress in plants. *Autophagy.* 5:954–963. http://dx.doi.org/10.4161/auto.5.7.9290

Ma, W., and G.A. Berkowitz. 2007. The grateful dead: Calcium and cell death in plant innate immunity. *Cell. Microbiol.* 9:2571–2585. http://dx.doi.org/10.1111/j.1462-5822.2007.01031.x

Marty, F. 1999. Plant vacuoles. *Plant Cell.* 11:587–600. http://dx.doi.org/10.1105/tpc.11.4.587

May, M.J., and C.J. Leaver. 1993. Oxidative stimulation of glutathione synthesis in *Arabidopsis thaliana* suspension cultures. *Plant Physiol.* 103:621–627. http://dx.doi.org/10.1104/pp.103.2.621

Meiri, D., and A. Breiman. 2009. *Arabidopsis* ROF1 (FKBP62) modulates thermotolerance by interacting with HSP90.1 and affecting the accumulation of HsfA2-regulated sHSPs. *Plant J.* 59:387–399. http://dx.doi.org/10.1111/j.1365-313X.2009.03878.x

Ohama, N., K. Kusakabe, J. Mizoi, H. Zhao, S. Kidokoro, S. Koizumi, F. Takahashi, T. Ishida, S. Yanagisawa, K. Shinozaki, and K. Yamaguchi-Shinozaki. 2016. The transcriptional cascade in the heat stress response of *Arabidopsis* is strictly regulated at the level of transcription factor expression. *Plant Cell.* 28:181–201.

Ozgur, R., I. Turkan, B. Uzilday, and A.H. Sekmen. 2014. Endoplasmic reticulum stress triggers ROS signalling, changes the redox state, and regulates the antioxidant defence of *Arabidopsis thaliana*. *J. Exp. Bot.* 65:1377–1390. http://dx.doi.org/10.1093/jxb/eru034

Pavet, V., E. Olmos, G. Kiddle, S. Mowla, S. Kumar, J. Antoniw, M.E. Alvarez, and C.H. Foyer. 2005. Ascorbic acid deficiency activates cell death and disease resistance responses in *Arabidopsis*. *Plant Physiol.* 139:1291–1303. http://dx.doi.org/10.1104/pp.105.067686

Pucciariello, C., V. Banti, and P. Perata. 2012. ROS signaling as common element in low oxygen and heat stresses. *Plant Physiol. Biochem.* 59:3–10. http://dx.doi.org/10.1016/j.plaphy.2012.02.016

Ramírez, L., C.G. Bartoli, and L. Lamattina. 2013. Glutathione and ascorbic acid protect *Arabidopsis* plants against detrimental effects of iron deficiency. *J. Exp. Bot.* 64:3169–3178. http://dx.doi.org/10.1093/jxb/ert153

Reape, T.J., and P.F. McCabe. 2008. Apoptotic-like programmed cell death in plants. *New Phytol.* 180:13–26. http://dx.doi.org/10.1111/j.1469-8137.2008.02549.x

Robert, N., I. d'Erfurth, A. Marmagne, M. Erhardt, M. Allot, K. Boivin, L. Gissot, D. Monachello, M. Michaud, A.-M. Duchêne, et al. 2012. Voltage-dependent-anion-channels (VDACs) in *Arabidopsis* have a dual localization in the cell but show a distinct role in mitochondria. *Plant Mol. Biol.* 78:431–446. http://dx.doi.org/10.1007/s11103-012-9874-5

Sandaklie-Nikolova, L., R. Palanivelu, E.J. King, G.P. Copenhaver, and G.N. Drews. 2007. Synergid cell death in *Arabidopsis* is triggered following direct interaction with the pollen tube. *Plant Physiol.* 144:1753–1762. http://dx.doi.org/10.1104/pp.107.098236

Schneider, A., T. Schatten, and H. Rennenberg. 1992. Reduced glutathione (GSH) transport in cultured tobacco cells. *Plant Physiol. Biochem.* 30:29–38.

Skouta, R., S.J. Dixon, J. Wang, D.E. Dunn, M. Orman, K. Shimada, P.A. Rosenberg, D.C. Lo, J.M. Weinberg, A. Linkermann, and B.R. Stockwell. 2014. Ferrostatins inhibit oxidative lipid damage and cell death in diverse disease models. *J. Am. Chem. Soc.* 136:4551–4556. http://dx.doi.org/10.1021/ja411006a

Sun, X., Z. Ou, M. Xie, R. Kang, Y. Fan, X. Niu, H. Wang, L. Cao, and D. Tang. 2015. HSPB1 as a novel regulator of ferroptotic cancer cell death. *Oncogene.* 34:5617–5625. http://dx.doi.org/10.1038/onc.2015.32

van Doorn, W.G., E.P. Beers, J.L. Dangl, V.E. Franklin-Tong, P. Gallois, I. Hara-Nishimura, A.M. Jones, M. Kawai-Yamada, E. Lam, J. Mundy, et al. 2011. Morphological classification of plant cell deaths. *Cell Death Differ.* 18:1241–1246. http://dx.doi.org/10.1038/cdd.2011.36

Van Hautegem, T., A.J. Waters, J. Goodrich, and M.K. Nowack. 2015. Only in dying, life: Programmed cell death during plant development. *Trends Plant Sci.* 20:102–113. http://dx.doi.org/10.1016/j.tplants.2014.10.003

Wahid, A., S. Gelani, M. Ashraf, and M.R. Foolad. 2007. Heat tolerance in plants: An overview. *Environ. Exp. Bot.* 61:199–223. http://dx.doi.org/10.1016/j.envexpbot.2007.05.011

Wind, S., K. Beuerlein, T. Eucker, H. Müller, P. Scheurer, M.E. Armitage, H. Ho, H.H. Schmidt, and K. Wingler. 2010. Comparative pharmacology of chemically distinct NADPH oxidase inhibitors. *Br. J. Pharmacol.* 161:885–898. http://dx.doi.org/10.1111/j.1476-5381.2010.00920.x

Xie, Z., and D.J. Klionsky. 2007. Autophagosome formation: Core machinery and adaptations. *Nat. Cell Biol.* 9:1102–1109. http://dx.doi.org/10.1038/ncb1007-1102

Yagoda, N., M. von Rechenberg, E. Zaganjor, A.J. Bauer, W.S. Yang, D.J. Fridman, A.J. Wolpaw, I. Smukste, J.M. Peltier, J.J. Boniface, et al. 2007. RAS-RAF-MEK-dependent oxidative cell death involving voltage-dependent anion channels. *Nature.* 447:864–868. http://dx.doi.org/10.1038/nature05859

Yang, W.S., and B.R. Stockwell. 2008. Synthetic lethal screening identifies compounds activating iron-dependent, nonapoptotic cell death in oncogenic-RAS-harboring cancer cells. *Chem. Biol.* 15:234–245. http://dx.doi.org/10.1016/j.chembiol.2008.02.010

Yang, W.S., R. SriRamaratnam, M.E. Welsch, K. Shimada, R. Skouta, V.S. Viswanathan, J.H. Cheah, P.A. Clemons, A.F. Shamji, C.B. Clish, et al. 2014. Regulation of ferroptotic cancer cell death by GPX4. *Cell.* 156:317–331. http://dx.doi.org/10.1016/j.cell.2013.12.010

Yang, W.S., K.J. Kim, M.M. Gaschler, M. Patel, M.S. Shchepinov, and B.R. Stockwell. 2016a. Peroxidation of polyunsaturated fatty acids by lipoxygenases drives ferroptosis. *Proc. Natl. Acad. Sci. USA.* 113:E4966–E4975. http://dx.doi.org/10.1073/pnas.1603244113

Yang, X., R. Srivastava, S.H. Howell, and D.C. Bassham. 2016b. Activation of autophagy by unfolded proteins during endoplasmic reticulum stress. *Plant J.* 85:83–95. http://dx.doi.org/10.1111/tpj.13091

Yoshida, H., Y.Y. Kong, R. Yoshida, A.J. Elia, A. Hakem, R. Hakem, J.M. Penninger, and T.W. Mak. 1998. Apaf1 is required for mitochondrial pathways of apoptosis and brain development. *Cell.* 94:739–750. http://dx.doi.org/10.1016/S0092-8674(00)81733-X

Zhang, M.-Y., A. Bourbouloux, O. Cagnac, C.V. Srikanth, D. Rentsch, A.K. Bachhawat, and S. Delrot. 2004. A novel family of transporters mediating the transport of glutathione derivatives in plants. *Plant Physiol.* 134:482–491. http://dx.doi.org/10.1104/pp.103.030940

Zheng, Z., S.A. Qamar, Z. Chen, and T. Mengiste. 2006. *Arabidopsis* WRKY33 transcription factor is required for resistance to necrotrophic fungal pathogens. *Plant J.* 48:592–605. http://dx.doi.org/10.1111/j.1365-313X.2006.02901.x

Distéfano et al., https://doi.org/10.1083/jcb.201605110

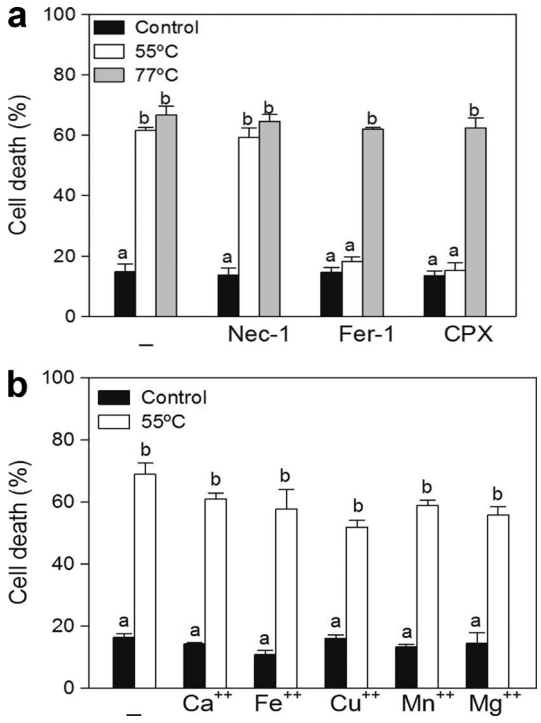

Figure S1. **Effect of the necroptosis inhibitor Nec-1 and divalent transition metal ions on cell death induced by a 55°C HS treatment.** (a) Effect of Nec-1 on cell death triggered by 55°C or a 77°C HS treatment. 6-d-old seedlings were preincubated overnight (16 h) with 20 µM Nec-1, 1 µM Fer-1, or 10 µM CPX. (b) 6-d-old seedlings were preincubated overnight (16 h) with different divalent transition metal ions as indicated. (a and b) Cell death was induced by treatment at 55°C for 10 min. Root hairs were stained with Sytox green, and dead root hairs were quantified. Results are expressed as a percentage of dead cells. Data are the mean ± SEM of three independent experiments. Different letters denote statistical difference (one-way analysis of variance, $P < 0.05$).

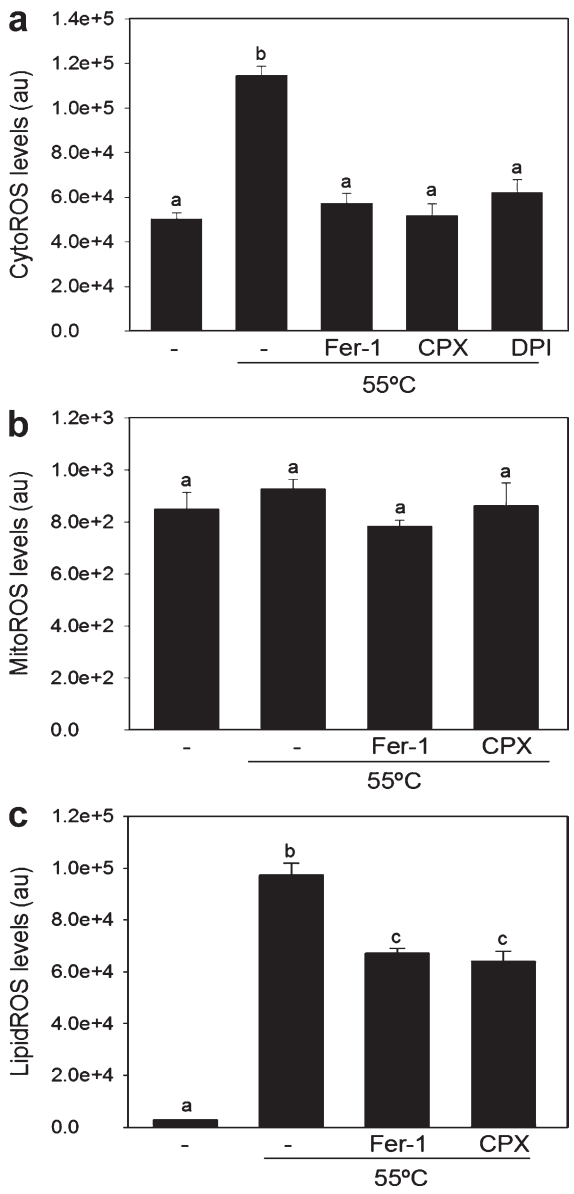

Figure S2. **55°C HS in *Arabidopsis* cell suspensions triggers the accumulation of ROS, which can be inhibited by Fer-1, CPX, and DPI.** 7-d-old cultures were pretreated overnight (16 h) with 1 µM Fer-1, 10 µM CPX, or 10 µM DPI as indicated and treated at the specified temperature. (a) Cytosolic ROS (CytoROS) levels were detected with the H2DCFDA probe 3 h after a 55°C treatment. (b) Mitochondrial ROS (MitoROS) levels were detected with the mitoSOX probe 3 h after a 55°C treatment. (a and b) Data are the mean ± SEM of three independent experiments. Different letters denote statistical difference (one-way analysis of variance, $P < 0.05$). (c) Lipid ROS levels were detected with the C11-BODIPY probe 3 h after 55°C treatment. Data are the mean ± SEM of three independent experiments. No significant differences were found (one-way analysis of variance).

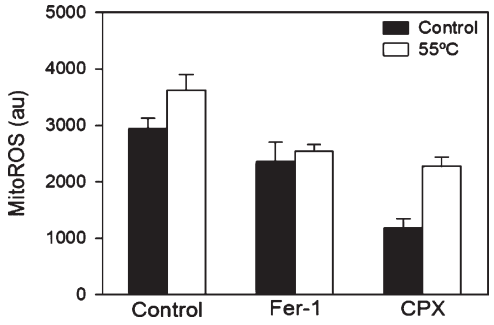

Figure S3. **MitoSOX is not involved in the cell death triggered by 55°C treatment in *Arabidopsis* root hairs.** Mitochondrial ROS (MitoROS) levels were detected with the mitoSOX probe 3 h after 55°C treatment. Data are the mean ± SEM of three independent experiments.

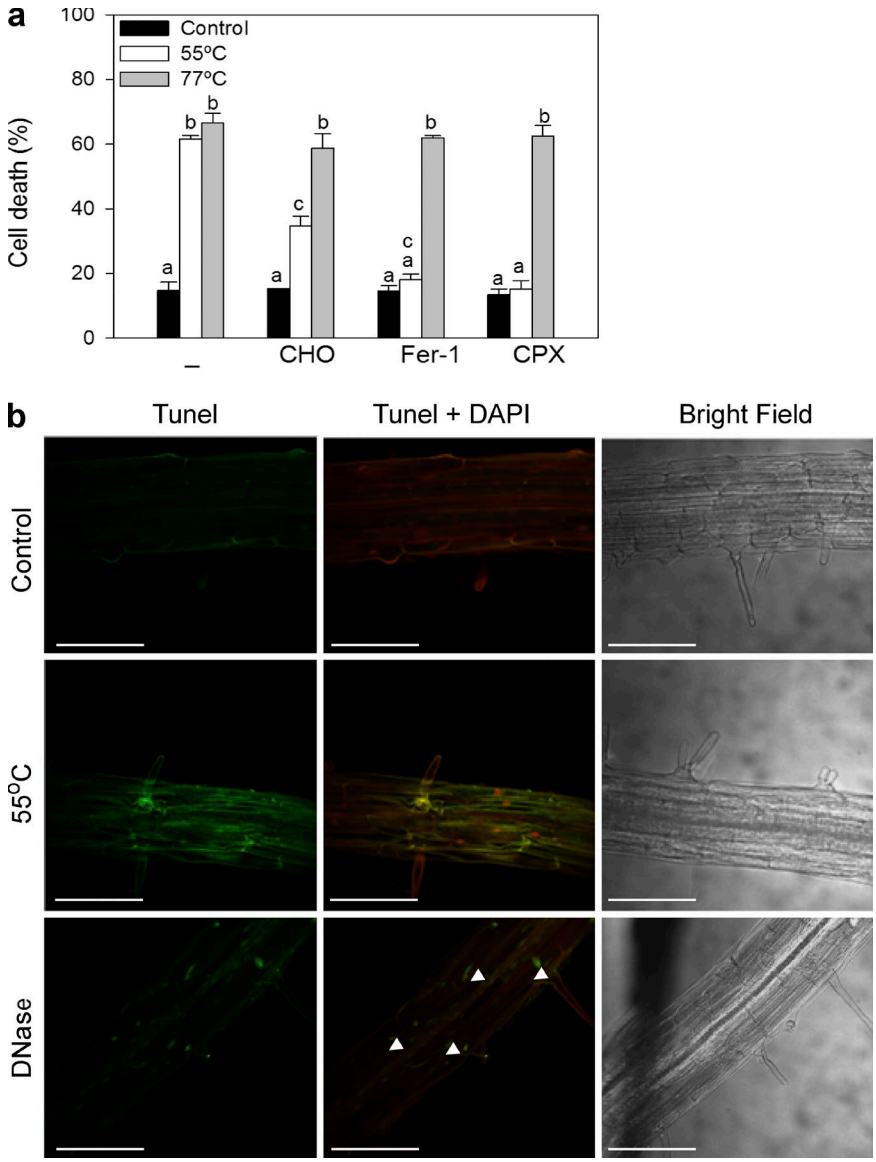

Figure S4. **A caspase-like activity is required for cell death after a 55°C HS, but DNA fragmentation is not detected.** (a) Effect of the caspase-3 inhibitor CHO on rates of HS-induced cell death in *Arabidopsis* root hairs. 6-d-old seedlings were preincubated in a 1 µM CHO solution or with 1 µM Fer-1 or 10 µM CPX for 16 h before HS at 55°C or 77°C. Root hairs were stained with Sytox green, and dead root hairs were quantified. Results are expressed as a percentage of dead cells. Data are the mean ± SEM of three independent experiments. Different letters denote statistical difference (one-way analysis of variance, $P < 0.05$). (b) TUNEL labeling of *Arabidopsis* roots showed no TUNEL-positive nuclei in roots submitted to 55°C HS. Arrowheads indicate positive TUNEL nuclei. Bars, 100 µm.

a

Treatment	Remaining spores	Only FM
Mock	4	118
CPX	6	119
Fer-1	4	108

b

Treatment	Fertilized ovules	Unfertilized ovules
Mock	64	17
CPX	59	12
Fer-1	62	21

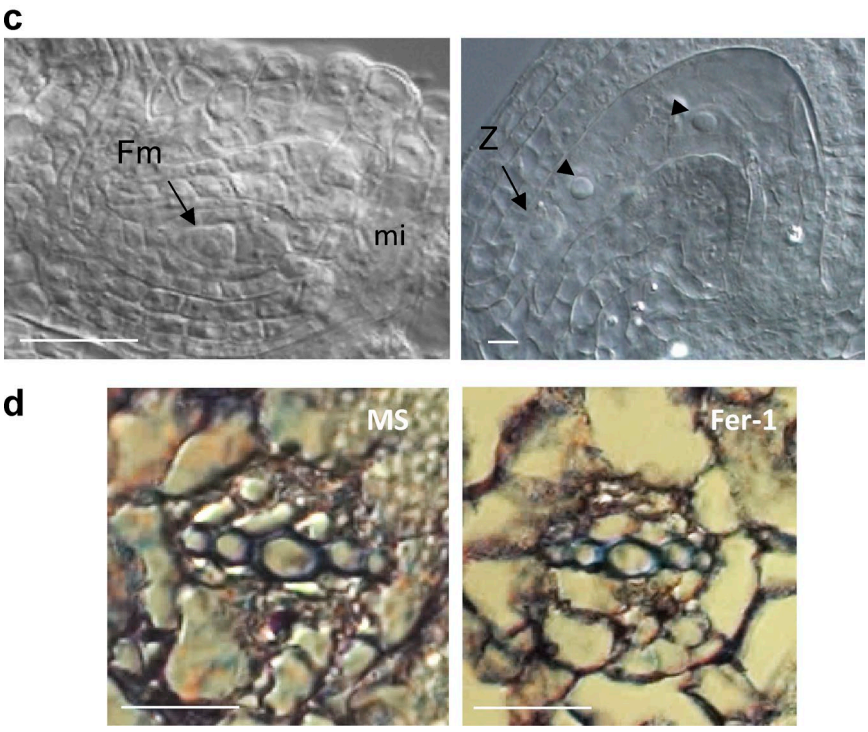

Figure S5. **Effect of ferroptosis inhibitors on reproductive and vascular development in *A. thaliana*.** (a) Megaspore cell death was analyzed in pistils from *Arabidopsis* inflorescences that were treated with either 10 μM CPX or 1 μM Fer-1 (in 0.1% DMSO and 0.01% Silwet L-77) or a mock solution (0.1% DMSO and 0.01% Silwet L-77). (b) Fertilization as a sign of normal synergid cell death was analyzed in pistils from *Arabidopsis* inflorescences that were treated with either 10 μM CPX or 1 μM Fer-1 (in 0.1% DMSO and 0.01% Silwet L-77) or a mock solution (0.1% DMSO and 0.01% Silwet L-77) that showed signs of pollination (pollen on the stigma) 3 d after treatment. (c) DIC images of a developing ovule showing a functional megaspore (Fm; left) and a fertilized embryo sac showing a zygote (Z) and endosperm nuclei (arrowheads). Mi, micropyle. Bars, 25 μm. (d) The effect of ferroptosis inhibitors on xylem anatomy was analyzed in hypocotyls of 6-d-old plants that were grown in Murashige and Skoog medium or alone or with 1 μM Fer-1. 50 plants were used for observations in each case. No differences were observed. Bars, 50 μm.

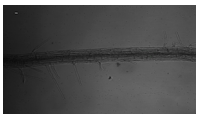

Video 1. **Sytox green staining of the different cell types that compose the root right after a 55°C HS treatment (T0).** The video is derived from a stack of serial confocal z sections taken through the root of a 6-d-old seedling stained with SYTOX green after a 55°C HS (4-μm step size). This video supplements Fig. 2 b.

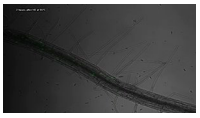

Video 2. **Sytox green staining of the different cell types that compose the root 2 h after a 55°C HS treatment.** The video is derived from a stack of serial confocal z sections taken through the root of a 6-d-old seedling stained with SYTOX green 2 h after a 55°C HS (4-μm step size). This video supplements Fig. 2 b.

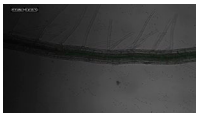

Video 3. **Sytox green staining of the different cell types that compose the root 4 h after a 55°C HS treatment.** The video is derived from a stack of serial confocal z sections taken through the root of a 6-d-old seedling stained with SYTOX green 4 h after a 55°C HS (4-μm step size). This video supplements Fig. 2 b.

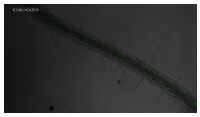

Video 4. **Sytox green staining of the different cell types that compose the root 6 h after a 55°C HS treatment.** The video is derived from a stack of serial confocal z sections taken through the root of a 6-d-old seedling stained with SYTOX green 6 h after a 55°C HS (4-µm step size). This video supplements Fig. 2 b.

Table S1. **Identity of the transcriptional pharmacodynamic ferroptosis markers reported in Dixon et al. (2014) and putative orthologues found in *A. thaliana***

Ferroptosis marker	Description	*Arabidopsis* blast hits (e value)
ChAC1	Mammalian proapoptotic protein of unknown function induced during endoplasmic reticulum stress	AT4G31290 (7e-30), AT1G44790 (2e-36), AT5G26220 (8e-28)
DDit4	DNA damage–inducible transcript 4	
LOC284561	Uncategorized gene affiliated with the lncRNA class	
Asparagine synthetase	Encodes asparagine synthetase (EC 6.3.5.4)	AT5G65010 (2e-115), AT3G47340 (2e-114), AT5G10240 (2e-114)
TSC22D3	Encodes for a leucine zipper protein, functions as transcriptional regulator	
DDIT3	DNA damage–inducible transcript 3	
JDP2	HUMAN isoform 2 of Jun dimerization protein 2	
SESN2 gene	Member of the sestrin family of PA26-related proteins	
SLC1A4	Solute carrier family 1 (glutamate/neutral amino acid transporter), member 4	
PCK2	Phosphoenolpyruvate carboxykinase 2 (mitochondrial)	
txnip	Encodes for a thioredoxin-interacting protein	
VLDLR gene	Encodes a lipoprotein receptor that is a member of the LDLR family	
GPT2 gene	Alanine aminotransferase: catalyzes the reversible transamination between alanine and 2-oxoglutarate to form pyruvate	AT1G72330.1, mitochondrion, 6e-150; AT1G23310.1 apoplast, chloroplast, cytoplasm, membrane, peroxisome, vacuole, 3e-147; AT1G70580.4 chloroplast, chloroplast, stroma, cytoplasm, peroxisome, 3e-145; AT1G17290.1 chloroplast, mitochondrion, 2e-142

Table S2. **List of primer pairs used for quantitative PCR**

Gene	Forward, 5′ to 3′	Reverse, 5′ to 3′
ASN1	GGGATGCAAGCTGGTCCAACA	TGACCCATCATCATCGGCATGT
ASN2	GCTGTAGAATGGGATGCAACTTGGT	TCCTCAATGCCTGTAGTGTTGTTCT
ASN3	ACGCAGCTTGGTCACAGAATCT	CCTCAAACAATGGCTGGAGTCTTCT
CCL1	TCAGGGCCAAACAGAGACTA	CGGTGGCATCAATGTCTAAC
CCL2	GGGCATGAGGAGGACTATGT	GGCTTGCTCTTGATTCCTTC
CCL3	CCAGCTCCATTGGAAGAAAT	TACTCTCGGTTGTTCCCACA
GPT2a	AGTTGTAGTCCCTGGTTCTGGCT	AGCTCTTGTGGAACTCTGTCAGACG
GPT2b	TCCCTTGCCTTCACCTTCCACA	AGCCAGAACCAGGGACAACGA
VDAC1	GAACGACAAGGGCGATCTAT	TAACTTGTGGCTCACTTCGG
VDAC2	GGCCCTTACGTCTACTGCTC	ACTTGTATTGGGTGGCAACA
VDAC3	GGCCCTGAAGTGGGTAGA	AAGATTGTTTAGCAAACCAGACA
VDAC4	ATCACAAGTCTGGCAAGCTG	ACAGAGGAGTTGGGTTGAGG
VDAC5	GGGTATGACACCACATCTCG	GGCTTTGATCGAATCTCCTT
KOD	TATGTGGTGGCTAGTTGGACTTACA	AGCTTTACTTAGAGATGACAGAGACGCT
BAX-1	CCCTTGATCAAAGTGGCAAT	GAAAGCAGTCCTCCAAGGTAGAG
HRD1	GCTCAAGGAAGGTCAATGGG	CAAGGGAAGGCCATAGTTCA
SEL1	GGAATATGCAGTCGAAGATGG	CACCGGAGAATCCTTTGAGA
PR2	GCAATGCAGAACATCGAGAA	TCATCCCTGAACCTTCCTTG
PR5	GCCGTGGAGCTAACGATAAG	GCGTAGCTATAGGCGTCAGG
WRKY33	TGGAGAGAGCATCACACGAC	GTGCTCTGTTTGTGGCGTAA
LSD1	TGTCAAACTACGAACCTTGTGC	TTGATCTGCGCAACCTGA
ACS2	GCTGGTTTATTTGCGTGGAT	AGGAAGAGCCAGGAGACACA
ATG7	TGTTACACGCCCGGGTCTAG	GAGTTCAACGGCGAGAGCTC
ATG8	ATTGTCGAAAGAGCCGAGAA	GATCCGCTTCCGTACAACAT
ATG9	AGACCCTTGAGTGGACCCTT	AGCCCAACCACAAATAGTCG
VPE	AAAGGTGGAAGCGGTAAGGT	TATGTGAGGCGTATTTGGCA
MC1	CCGAGGAAGAAACTGATCCA	GTTTCTTTGACGCGAACCAT
MC2	CGTGGACGATGAGATCAATG	TCCGAGCCTGTCCATTCTAC
RHD6	CCTAAATCCGCTGGAAACAA	TGTTGGCTTAGGCTTGGTCT
WER	GCTCCACAAGTTGCTTGGTA	TCACCATTGCTCTGTTTGGT
Bip1	TGCCTTTGAGCATCATTGAA	TCAGTCCTGAGGAGATTAGTGCT
Bip2	TCTCCTCAGGACTGAAAACCT	TCGACGTTAAGAGATTGATCG
Bip3	GGCTTCCCATCTTTGTTCAC	CGAAACGTCTGATTGGAAGAA
Bzip60	TCTCAAGCATTCTCTTTCGAGAT	CGATGATGCTGTGGCTAAAA